



Effects of coupled heat sources in a triple power cycle: thermodynamic, economics and environment analysis and optimization

Mahdi Alibeigi¹ · Somayeh Davoodabadi Farahani¹ · Sina Amiri Hezaveh¹

Received: 12 April 2021 / Accepted: 13 October 2021 / Published online: 22 October 2021
© The Author(s), under exclusive licence to Islamic Azad University 2021

Abstract

In this study, the thermodynamic and economic analysis for a triple combination including the Brayton cycle (GT), reheat cycle and an organic Rankine cycle, and Brayton cycle by coupling geothermal with biomass energy source and solar energy source is presented. Thermodynamically and economically, the effects of changing working fluid, air, CO, CO₂, N₂, and NO₂ are studied for pressure ratio and air mass flow in the GT. The highest and lowest total thermal efficiency belong to CO and NO₂ with values of 32.98% and 30.64%, respectively. The highest thermal efficiency and the lowest cost occur in the pressure ratio of 4 and 2, respectively. Ammonia and isopropanol have the highest and lowest combined power output cycles with organic Rankine cycle efficiency of 0.8654 and 0.9499, and amount of the overall thermal efficiency equal to 0.4196 and 0.4067, respectively. In addition, geothermal energy, solar energy, and biomass energy have been used to supply part of the energy required by the cycle. The solar tower is designed to supply the required heat from the sun. Optimization is performed based on thermal efficiency and cycle cost using a genetic algorithm. The solar thermal efficiency of summer was less than winter, and the cost of heat source in summer was more than winter because of the expense of geothermal in summer. Compared to the geothermal–solar cycle, the geothermal–biomass cycle has a lower cost and better performance. The environmental effects of the cycle have been investigated with different energy sources, and it has been found that the geothermal–solar cycle has less destructive ecological impacts.

Keywords Solar energy · Geothermal · Biomass · RC-GT-ORC · Emission

Introduction

Access to energy is one of the most fundamental components of development in societies. Therefore, a sufficient and reliable source of energy is the need of every society of its which developed and evolving. On the other hand, the growing consumption of fossil fuels has led to the emission of greenhouse gases, global warming, and environmental damage. Over the past two decades, the rise in energy prices and environmental damage, the limited resources of renewable energy, and the use of maximum energy-efficient have become increasingly important [1].

Gaining energy for electricity generation has customarily been supplied from fossil fuels, where the fuel can be stored for instant access to energy when required, representing, stable form of energy.

The share of electricity generation by source in the world is as follows by 2014 in the USA (United States of America): coal (39%), oil (1%), natural gas (27%), nuclear (19%), hydro (6%), solar/wind (5%), and biofuel (2%). Therefore, the research and optimization of steam cycles are significant due to the old design of some power plants (non-compliance with modern technology) and their largest share in electricity generation. Newly, Brayton cycle (BC) operating with working fluid in higher than critical pressure as one of the power productions cycles has been thought about more than ever, is the [2].

The biomass and geothermal renewable energy sources are willingly accessible stable forms of energy to store of its. If suitable storage methods can be innovated, recurrent renewable energy sources such as biomass and geothermal

✉ Somayeh Davoodabadi Farahani
sdfarahani@arakut.ac.ir

¹ Department of Mechanical Engineering, Arak University of Technology, Arak 38181-46763, Iran

power can replace fossil fuels in a sustainable energy grid. This also suggests enhanced efficiency as maximum requiring, which conventionally has led to over-designed and expensive power plants completed working at steady-state manufacture much higher than the average baseload electricity requiring. The main criteria of electrical energy storage technologies are applied to use pumped hydroelectric storage (UPHES), compressed air energy storage, battery, flow battery, fuel cell, solar fuel, superconducting magnetic energy storage, flywheel, capacitor/supercapacitor, and thermal energy storage to use in the petroleum refinery or power plant [3, 4].

Lately, the low thermal efficiency of BC and Rankine cycle is the cause of attending to combine cycles. Some work has been done in this regard. Burer et al. [5] analyzed the efficiency of a triple plant by combining the (SOFC) system and the gas turbine as the primary stimulus. Al-Sulaiman et al. [6] presented a comprehensive study of the triple system based on the initial stimulus of the steam turbine and the use of the organic Rankine cycle (ORC) at different temperatures from energy sources. The temperature is between 15° and 55° for the lowest source temperature, and the average temperature is between 150 and 300 Celsius, also the highest temperature is around 300 Celsius; then, it has been examined the amount of efficiency and productivity. Finally, they showed when the energy source reaches maximum temperature of its, the organic Rankine cycle (ORC) could achieve maximum efficiency. Wang et al. [7] studied the ORC and the dense vapor cycle for the production of cooling and heating and their effects on the cycle efficiency. Wu et al. [8] conducted a study on the combination of ORC and high-density vapor cycle, in which the organic cycle uses heat from other sources. They found the efficiency increased to 66%. Khan et al. [9] presented an analysis of two cycles combination including partial heating supercritical CO_2 (PSCO₂) cycle and ORC by changing organic fluid and variation working fluid of PSCO₂ cycle for finding thermal efficiency, exergy efficiency, and exergy destruction with effects of solar irradiance and the inlet pressure of SCO₂ turbine. Habibi et al. [10] studied a cascade power generation system, involving a partial evaporation Rankine cycle (PERC) has been used instead of a conventional steam turbine, a screw expander, and using an organic Rankine cycle (ORC) with a storage tank coupled with a parabolic trough solar collector (PTSC) to drive storage tank has been optimized for energy and exergoeconomic. Liu et al. [11] presented the optimum exergoeconomic efficiency of a combined supercritical carbon dioxide recompression Brayton/organic flash cycle. The shortage of fossil fuels and the gradual rise in its price on the one hand and environmental pollution on the other hand have made the use of medium- or low-temperature energy sources particularly important. Meanwhile, Rankine's organic cycle technology

could play an important role. This cycle is similar to that of the Rankine cycle, except that organic fluids are used instead of water. Due to the low critical temperature of organic fluids relative to water, Rankine's organic cycle, unlike Rankine's vapor cycle, was able to use low-temperature heat sources, including heat dissipation in industry or heat from renewable energy sources such as solar, earth heat, and biomass. The size of (ORC) systems is usually a few 100 kw, which is much smaller than conventional steam cycles. These systems use evaporators for boilers. The other components of the cycle are similar to those of the Rankine cycle. At last, heat or low-grade heat is used in the evaporator to evaporate organic fluids. This high-pressure steam in the turbine increases and produces power. The low-pressure steam at the turbine outlet is distilled in the condenser. The working fluid is pumped back to the evaporator, and the cycle is reiterated. Choosing the right work fluid can greatly improve the performance of such a cycle. Unlike mixed fluids, there have been many studies on pure fluids. Due to the study of mixed fluids in the present study, only a few cases of research with pure fluids are mentioned.

Tempesti et al. [12] simulated synchronic heat production and work on a micro-scale using simultaneous geothermal and solar energy from energy, exergy, and economic perspective. Mohammadkhani et al. [13] presented a thermo-economic analysis for the combined cycle.

Liu et al. [14] examined several fluids at different evaporator temperatures and found that the evaporator efficiency would be maximal when fluids with lower evaporation enthalpy were used. Mikielewicz and Mikielewicz [15] examined the thermodynamic and functional properties of several fluids in supercritical and subcritical states to apply heat and power production in domestic use. The results showed that of the 20 studied fluids, ethanol, R141b, and R123 were more suitable for the mentioned application. Also, cycles that used fluids in the supercritical state gained about 5% more than cycles in which the fluids are below the critical state; but they needed more compact and efficient converters. Dai et al. [16] studied the use of ten different fluids on cycle performance and concluded that under the conditions considered, adding an internal heat exchanger does not help to improve cycle performance, as well as for fluids whose slope of the saturated steam curve is the $(T - S)$ chart is not negative, the superheating of the fluid will not increase the efficiency, and among the studied fluids, R236fa was introduced as the most suitable fluid. Extended cycles have been used to increase the efficiency and power of the gas turbine cycle. Among them, reheat includes a second heat addition in the basic gas path, downstream of the main combustor. The cycle uses two turbines that operate at high and low pressures. The structure, as mentioned, can operate in different



thermal and pressure bases to use the minimum energy lost in obtaining power.

Sirignano and Liu [17] and Maksoud [18] suggest an ongoing combustion all over the turbine for concurrent expansion and heat addition, leading to near-constant temperature combustion. A concept with more practical relevance notices one or multi-fuel discrete reheats along the expansion part, and it has been studied. Energy resources are needed to supply power of a power plant cycle, also fossil fuels destroy the environment, and cause increasing greenhouse gases, and ultimately destroying the ozone layer and acid rain. Environmentalists are using renewable sources such as solar, biomass, and geothermal, which are discussed here [19]. The design parametric of solar energy is great motivation in the new studies [20, 21]. The consolidation of solar energy and thermal power cycle such as the Brayton cycle is an emerging technique characterized by higher thermal efficiency at the design solar power (CSP) system temperature range. Focus on solar power is one of the most promising makes renewable electricity production. This is the station on its capacity to reservoir large quantities of thermal energy at medium cost and for these causes. It has attracted the attention of government officials and researchers [22–26]. Other renewable energy sources include biomass. Biomass energy is one of the most suitable renewable energies that has been used in the past cause of being environmentally compatible [27]. Each year, through photosynthesis, the amount of solar energy stored in the leaves, trunks, and branches of trees is equivalent to several times the world's annual energy consumption. However, among a variety of renewable sources, biomass is highly rated for solar energy. Another renewable energy is geothermal. Geothermal energy plays an important role in the world's energy supply. Due to many advantages of its over fossil fuels or even some renewable energy in some areas, it can be quite cost-effective. Today, heat reservoirs are used in two main ways: direct use of thermal energy and indirect use of electricity generation [28]. Since source of its does not depend on weather conditions, ground generation power plants usually operate more than 70% (up to 95% for new power plants) [29].

Simultaneous use of geothermal and solar energy sources was done in 2006 and has yielded promising results in the field of economics and energy supply [30]. Boyaghchi and Heidarnejad [31] simulated a cycle of simultaneous production of power, heat, and refrigeration with the stimulation of solar energy, exergy. With combination regenerative Brayton and inverse Brayton cycles by varying the cycle parameters, power and efficiency have been optimized [32]. A new triple cycle and gas turbine that conducts excess heat of carbon dioxide (s-CO₂) under different operating conditions, optimized by the Particle Swarm Optimization (PSO) algorithm by MATLAB software. The target functions are the overall

thermal efficiency and surface electricity costs (LCOE). In the optimal state, the overall thermal efficiency and leveled cost of electricity (LCOE) are 0.521, and \$52.819/MWh, respectively [33]. Energy and exergy analysis for performance of organic Rankine cycle (ORC) with nine fundamental process parameters has been optimized by using Taguchi method to find the optimal level of each parameter, and also ANOVA method has utilized to gain objective functions for impact weights of each parameter and gray relational analysis method (GRA) for multi-objective of ORC characteristics [34].

Due to generating electricity, the utility of using combine cycle with renewable energy is important for storing the energy. The renewable energy can be applied to use to pumped hydroelectric storage (UPHES), compressed air energy storage, battery, flow battery, fuel cell, solar fuel, superconducting magnetic energy storage, flywheel, capacitor/supercapacitor, and thermal energy storage to use in the petroleum refinery or power plant.

In this study, the thermodynamic and economic analysis for a triple combination, including reheat cycle and an organic ranking cycle (ORC) and Brayton with different energy sources with various heat sources, is investigated. The various heat sources are biomass, geothermal, and solar energy. The geofluid temperature changes for finding design temperature for a suitable supply temperature of getting heat from geothermal have been considered. The effect of input mass flow rate on each cycle, pressure ratio, and use of organic cycle on efficiency and output power, and cost have been investigated. In addition, this paper tried to discuss the ecological impacts of various energy supply sources for energy production in power plants (organic ranking cycle (ORC) and Brayton), cost of cycle consumption, and energy resources.

The main objective criteria of this study are the improvement of renewable energy with each other as a new couple heat source such as biomass/geothermal source, and solar/geothermal source. In this regard, the value of these variables has been investigated to achieve the best performance of the combined cycle. Using the genetic algorithm, the optimal value for the effective parameters is determined based on the objective functions, namely thermal efficiency and cost. Pollutant emissions are estimated in the optimal state of the cycle.

Problem description and modeling

In this research, a triple combination of reheat cycle and an organic Rankine cycle (ORC) and Brayton with different energy sources with various heat sources is considered as shown in Fig. 1. This design has been done to exploit power generation as much as possible. According to Fig. 1,

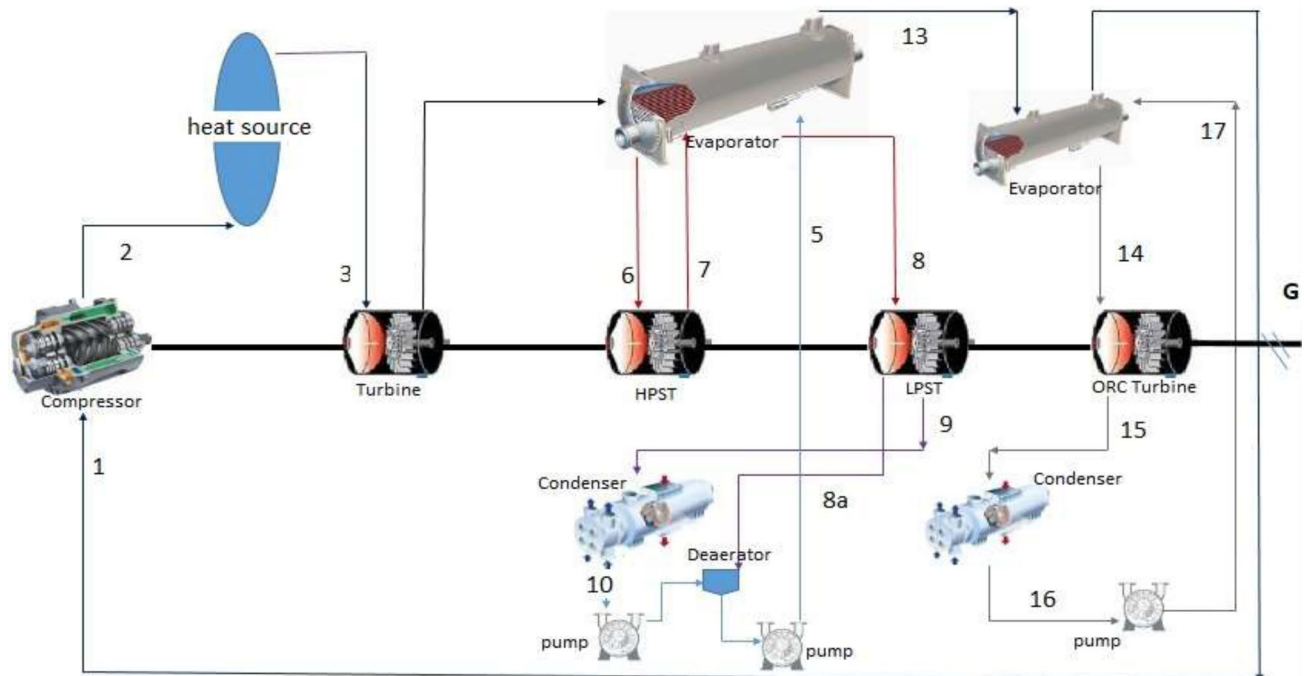


Fig. 1 Schematic of the proposed cycle

this cycle has 17 components, and the descriptions of each section are completely below. Path 1–2: At the state (1) entity entrance, air is being compressed to a higher pressure and higher temperature in the compressor, and air in high pressure and temperature conduces to the molten salt heat exchanger absorber. Path 2–3: In the molten salt heat exchanger, heat is gained by the high temperature and high-pressure air for expanding to the gas turbine in the state (4). Path 3–9: After the air is entered in the gas turbine (GT), the moderate temperature of the air with low pressure passes complete heat recovery steam turbine (HRSG) where the relationship between pressure and temperature calculated by the polytropic efficiency for the turbine and the passive low pressure in HRSG with superheated steam which has been exchanged by water carried reheat steam Rankine cycle to the feed pump at state (5). The superheated steam leaves heat recovery at a high temperature hence it comes into the high-pressure steam turbine at state 6 where the departure vapor at state (7) enters to state (8) for reheating, therefore in low-pressure steam turbine with steam bleeding facilities deaerated with the water at state (8a). In a low-pressure steam turbine (LPST), it is expandable to state (9) and then goes on to the next cycle which is the steam Rankine cycle at state (10) in the condenser. The steam turbine delivery for reheating of steam in HRSG exists between high-pressure steam turbine (HPST) and LPST. The superheated steam enters HPST at state (6) to (7) expanded thus, leading to reheating before being led to LPST at state (8). A fraction of steam is bled from LPST at state (8a) for feed heating, and deaeration and

the remaining steam expand to state (9). Path 10–17: After the steam expanded in LPST to state (9), it enters to state (10) in the Rankine cycle into the condenser of it where the heat is lost to the incoming cold water to deliver hot water for the procedure of heating and condensation for extracting to the pump at state (11). Thus, the evacuated water is delivered to HRSG at state (12), which is used by the feed pump. In HRSG, the air leaf for entrance to a heat exchanger is characterized as heat recovery vapor generator (HRVG) at state (13). In this state, the organic fluid R245fa is heated, where the organic fluid was heated by HRVG transformed to vapor for the entrance of the ORC turbine at state 14. The vapor expanded up to state (15) for producing work in ORC turbine where the organic fluid vapors left it. The departure organic fluid vapors enter the ORC condenser, and phase changes to saturated liquid form at state (16). Then, it transported to HRVG and for using the heating in ORC pump at state (17). The required air from state (13) evaporated for entering the HRVG at the cycle goes on and returns to the state (1). The inlet parametrical information for this combined cycle is given in Table 1. Also, the input parameters for each state are given in Table 2.

The schematic of the cycle is indicated for each component and path of each state in Fig. (1).



Table 1 Thermodynamical input parameters for investigation [35–37]

Parameter	Symbol	Values, unit
Ambient temperature	T_1	300, K
Ambient pressure	P_1	101.1, kPa
Exit pressure of air at GT cycle	P_4	121.32, kPa
Inlet pressure of air at GT cycle	P_{13}	111.21, kPa
Pressure loss in HRSG and HRVG	$P_{\text{loss, HRSG}} = P_{\text{loss, HRVG}}$	0.1% of, kPa
Effectiveness of HRSG	ϵ_{HRSG}	0.9
Effectiveness of HRVG	ϵ_{HRVG}	0.9
HP steam pressure	P_6	5560.5, kPa
HP steam temperature	T_6	600, K
LP steam pressure	$P_7 = P_8$	2022, kPa
Condenser pressure of SRC	P_9	5.055, kPa
LP steam reheat temperature	T_8	600, K
ORC turbine inlet pressure	P_{14}	404.4, K
ORC turbine inlet temperature	T_{14}	443, K
ORC condenser Temperature	T_{15}	313, K
Polytropic efficiency of the compressor	$\eta_{p,c}$	0.92
Polytropic efficiency of the turbine	$\eta_{p,T}$	0.86
Isentropic efficiency of steam turbine	$\eta_{T, \text{HPST}} = \eta_{T, \text{LPST}}$	0.8
ORC expander isentropic efficiency	η_{TORC}	0.8

Table 2 Input parameters for each state [38]

State no	\dot{m} (kg/s)	T (K)	P (kPa)
1	10	300	101.1
2	10	770.69	2426.4
3	10	1266.63	2426.4
4	10	626.68	121.32
5	0.645	430.7	5055
6	0.645	600	5055
7	0.645	500.64	2022
8	0.645	600	2022
8a	0.645	417.28	121.32
9	0.645	361.25	5.055
10	0.645	305.87	5.055
11	0.645	305.87	121.32
12	0.645	377.78	121.32
13	10	450	111.21
14	4.38	443	404.4
15	4.38	313	101.1
16	4.38	313	101.1
17	4.38	313.22	404.4

Thermodynamic modeling

This section explains the equations and relationships governing this cycle in the first and second laws of thermodynamics. Noticeably, the pressure drops, kinetic energy, potential energy, and heat dissipation have been neglected.

The energy balance equations for different parts of the cycle are written as (1, 2):

$$\sum \dot{m}_i = \sum \dot{m}_o \tag{1}$$

$$\dot{Q} - \dot{W} = \sum \dot{m}_o h_o - \sum \dot{m}_i h_i \tag{2}$$

According to the second law of thermodynamics, for all components, exergy analysis in SI unit (kJ/kg) is applied in any state component described by (3):

$$\psi = (h - h_0) - T_0(s - s_0) \tag{3}$$

The relationship between the temperature and pressure is given by (4) as polytropic efficiency and principal in the compressor:

$$\frac{T_2}{T_1} = \left(\frac{P_2}{P_1} \right)^{\left[\frac{\gamma-1}{\gamma \eta_{p,c}} \right]} \tag{4}$$

By changing enthalpy in the compressor, the power of the compressor is given in Eq. (5), and the specific work of the compressor is defined as (6):

$$W_{\text{COMP}} = \dot{m}_a (h_2 - h_1) \tag{5}$$

$$\dot{W}_{\text{COMP}} = \frac{W_{\text{COMP}}}{\dot{m}_a} \tag{6}$$

Air is used with a molar composition of 21% oxygen and 79% 183 nitrogen. The specific heat of air as a function of temperature in (kJ/kg–K) is given by (7) [39],

$$C_p = c_1 + c_2 T + c_3 T^2 + c_4 T^3 \quad (7)$$

where constant on the following equation must be set as $c_1 = 0.999638438$,

$$c_2 = -0.055205312 \times 10^{-3}, \quad c_3 = 0.346320281 \times 10^{-6}, \\ c_4 = -0.140118997 \times 10^{-9}.$$

In the molten salt heat exchanger, heat is gained by the high temperature and high pressure, which has been defined by (8):

$$\dot{Q} = \int_{T_2}^{T_3} \dot{m}_a \cdot C_p(T) \cdot dT \quad (8)$$

The exhaust temperature in the turbine is defined by the relationship between temperature and pressure ratio in the gas turbine with identification of the polytropic efficiency for the turbine given in Eq. (9), and the generative work in gas turbine is defined by changing enthalpy in the turbine in Eq. (10) and specific work in turbine defined in Eq. (11):

$$\frac{T_4}{T_3} = \left(\frac{P_4}{P_3} \right)^{\left[\frac{\gamma-1}{\gamma} \right] \eta_{p,T}} \quad (9)$$

$$W_{\text{TUR}} = m_a (h_3 - h_4) \quad (10)$$

$$\dot{W}_{\text{TUR}} = \frac{W_{\text{TUR}}}{m_a} \quad (11)$$

The produced work by HPST and LPST are given as (12), and (13), respectively:

$$W_{\text{HPST}} = m_w (h_6 - h_7) \quad (12)$$

$$W_{\text{LPST}} = m_w (h_8 - h_{8a}) + m_w (1 - f_r) (h_{8a} - h_9) \quad (13)$$

Also, the specific works of HPST and LPST are assumed as (14, 15):

$$\dot{W}_{\text{HPST}} = \frac{W_{\text{HPST}}}{m_w} \quad (14)$$

$$\dot{W}_{\text{LPST}} = \frac{W_{\text{LPST}}}{m_w} \quad (15)$$

where f_r is the steam-bled friction of these components, which its value is assumed to be 0.2. For each turbine, the second law efficiency is defined. The second law efficiency of HPST and LPST are assumed as:

$$\eta_{2\text{nd,HPST}} = \frac{\dot{W}_{\text{HPST}}}{\psi_6 - \psi_7} \quad (16)$$

$$\eta_{2\text{nd,LPST}} = \frac{\dot{W}_{\text{LPST}}}{\psi_8 - \psi_9} \quad (17)$$

where m_w is the mass of steam generated per (kg) of air in the following equations:

$$\eta_{2\text{nd,TUR}} = \frac{\dot{W}_{\text{TUR}}}{\psi_3 - \psi_4} \quad (18)$$

$$\eta_{2\text{nd,HRSG}} = \frac{\dot{m}_w \cdot (\psi_6 - \psi_5)}{\dot{m}_a \cdot (\psi_4 - \psi_{13})} \quad (19)$$

The organic Rankine cycle work of the pump is defined as (20):

$$W_{\text{PUMP,ORC}} = \dot{m}_r \cdot (h_{17} - h_{16}) \quad (20)$$

Individually, the specific work output is defined for each cycle such as the steam Rankine cycle, Brayton cycle, organic Rankine cycle, and reheat in the Rankine cycle.

The specific work output for the steam Rankine cycle is defined as follows (21):

$$\dot{W}_{\text{ST}} = (\dot{W}_{\text{HPST}} - \dot{W}_{\text{LPST}}) - \left(\frac{W_P + W_{\text{FP}}}{m_a} \right) \quad (21)$$

The specific work output for the Brayton cycle is explained as (22):

$$\dot{W}_{\text{GT}} = \dot{W}_{\text{TUR}} - \dot{W}_{\text{COMP}} \quad (22)$$

The specific work output for organic Rankine cycle is defined as (23):

$$\dot{W}_{\text{ORC}} = \frac{W_{\text{TUR,ORC}} - W_{\text{PUMP,ORC}}}{m_a} \quad (23)$$

The net specific work output for the overall combination cycle is the summation of specific work of each cycle. Therefore, it is defined as (24):

$$\dot{W}_{\text{Net}} = \dot{W}_{\text{GT}} + \dot{W}_{\text{ST}} + \dot{W}_{\text{ORC}} \quad (24)$$

Also, the thermal efficiency for each cycle is defined by the specific work and difference enthalpy of the basic component of the cycle. The thermal efficiency for the Brayton cycle is defined by (25):

$$\eta_{\text{GT}} = \frac{\dot{W}_{\text{GT}}}{(h_3 - h_2)} \quad (25)$$

The thermal efficiency for the reheat Rankine cycle is given by (26):

$$\eta_{SRC} = \frac{\dot{W}_{ST}}{(h_4 - h_{13})} \tag{26}$$

The thermal efficiency for organic Rankine cycle is determined by (27):

$$\eta_{ORC} = \frac{\dot{W}_{ORC}}{(h_{13} - h_1)} \tag{27}$$

The overall thermal efficiency of the combination of Brayton, reheat Rankine, and organic Rankine cycles is assumed as (28):

$$\eta_{overall} = \frac{\dot{W}_{Net}}{\dot{Q}_{in}} \tag{28}$$

The work fraction named as back-work ratio, which defined the power of the generative component divided by the power consumption component for each independent cycle orderly, Rankine cycle, and organic cycle, is considered as follows in Eqs. (29–31),

$$BWR_{GT} = \frac{W_{COMP}}{W_{TUR}} \tag{29}$$

$$BWR_{ST} = \frac{W_P + W_{FP}}{W_{HPST} + W_{LPST}} \tag{30}$$

$$BWR_{ORC} = \frac{W_{PUMP,ORC}}{W_{TUR,ORC}} \tag{31}$$

with a combination of three independent cycles including Rankine cycle, organic Rankine cycle, and Brayton cycle with feed heat from three ways of geothermal, solar, and biomass.

Geothermal

Geothermal energy is the thermal energy contained in the Earth’s solid crust. This type of energy is often used to generate geothermal electricity, which refers to the cycle of generating electrical energy from geothermal energy. The technology used in power generation projects includes geothermal power plants, dry steam power plants, fluid steam power plants, and dual cycle power plants. Geothermal energy is one of the renewable energy sources that has been considered in recent years because geothermal energy is a low-temperature energy source that can be used in the cycle of organic Rankine cycles. The geothermal consumption heat transfer is defined as, [40]

$$\dot{q}_{geo} = \dot{m}_{geo} c_{p,geo} \delta T_{geofluid} \tag{32}$$

$$\delta T_{geofluid} = (T_{geo,supply} - T_{geo,return}) \tag{33}$$

where $T_{geo,supply}$ and $T_{geo,return}$ are the geothermal fluid entering the absorber and the geothermal fluid returning to the injection well, respectively. The difference of $T_{geo,supply}$ and $T_{geo,return}$ is delivered in Eq. (33) as geofluid difference temperature, depending on the geothermal design temperature.

Besides, the dead point temperature for geothermal must be defined as the dry bulb temperature at the stage of installation of the geothermal. Thus, the theoretical maximum efficiency is Carnot efficiency defined for geothermal sources in Eq. (35):

$$T_0 = T_{db}, P_0 = P_{atm} \tag{34}$$

$$\eta_{carnot} = 1 - \frac{T_0}{T_{geo,supply}} \tag{35}$$

In act of city gate station (CGS), geothermal destroys the environment with emissions of destructive gases such as CO₂ because of low thermal efficiency. In order to use the natural gas (NG), the emission factor of CO₂ will be 0.179 ton CO₂/MWh in Iran. Moreover, it emitted methane (CH₄) and nitrogen oxide (NO₂) with emission factors 0.00341 and 0.000341 kg/MWh. [41]

Solar

The thermal modeling for the solar source in this case is considered by a hollow receiver based on the modeling done by Lee [42, 43] with a solar tower, which has been divided by numerous parts for concluding heat losses in each section, therefore deliberated the heat, which has been gained by absorber by the fluid. Although the energy of the receiver in the central of the receiver was not completely absorbed, and some of them, which received energy has been lost by conductive, convection (both forced convection and natural convection), emission, and reflection, where the summation of this losses gained the total heat losses, are defined as Eq. (36) [44]:

$$\dot{Q}_{loss} = \dot{Q}_{em} + \dot{Q}_{cond} + \dot{Q}_{conv} + \dot{Q}_{ref} \tag{36}$$

Consequently, the absorbing heat is explained by subtracting to receive heat and heat loss energies which is written as follows in Eq. (37):

$$\dot{Q}_{abs} = \dot{Q}_{rec} - \dot{Q}_{loss} \tag{37}$$

where in Table 3, it is noticed that ρ_s is density, F_r is the view factor of the receiver, $A_{sur}(m^2)$ is the surface area of the surrounding, $T_{in}(K)$ is the temperature of the inlet of the receiver, $T_{air}(K)$ is the temperature of the air in this condition inside of the receiver, ϵ is the emissivity of the receiver,

Table 3 The condition of the solar tower

ρ_s	F_r	$A_{sur}(m^2)$	$T_{in}(K)$	$T_{air}(K)$	ϵ
0.04	0.8	0.15	290	565	0.7
$k_{tube}\left(\frac{W}{mK}\right)$	$k_{insu}\left(\frac{W}{mK}\right)$	$\delta_{insu}(m)$	$d_o(m)$	$t(mm)$	$L_c(m)$
9.23	15	0.07	0.19	0.41	6

$k_{tube}\left(\frac{W}{mK}\right)$ is the thermal conductivity of tube, $k_{insu}\left(\frac{W}{mK}\right)$ is the thermal conductivity of insulation in the collector, $\delta_{insu}(m)$ is the thickness of insulation, $d_o(m)$ is the outlet diameter of the tube, $t(mm)$ the thickness of the tube, and $L_c(m)$ is the length of the collector.

Table 3 presents the condition of the definition of the solar tower

The heat transfer natural convection coefficient is explained for both sides of the receiver in which the natural heat transfer convection coefficient for inside the receiver is defined in Eqs. (34, 35) as [43],

$$\lambda_{air,nc,insi} = 0.81(T_{sur} - T_{air,nc,insi})^{0.426} \quad (38)$$

$$T_{air,nc,insi} = (T_{sur} + T_0)/2 \quad (39)$$

where $h_{air,nc,insi}$ is equal to the temperature of the inside of the receiver. The natural heat transfer convection coefficient for the outside of the receiver is assumed by (40):

$$\lambda_{air,nc,o} = 1.24(T_{insu} - T_0)^{1/3} \quad (40)$$

In a flat plate equal to the aperture occurred the forced convective heat loss. It considered the calculating amount of $\lambda_{air,fc,insi}$ from Nusselt number which is defined as (41):

$$Nu_{air,fc,insi} = 0.0287Re_{air,insi}^{0.8} Pr_{air,insi}^{1/3} \quad (41)$$

In addition, the Nusselt number, which is explained in the equation, can calculate the force convective coefficient outside the receiver (42):

$$Nu_{air,fc,o} = 0.0278913Re_{air,o}^{0.805} Pr_{air,o}^{0.45} (0.785T_{insu,w}/T_0)^{0.2} \quad (42)$$

On the whole, the total convective heat transfer coefficient air is considered by (43):

$$\lambda_{air,0} = \left(\lambda_{nc,o}^a + \lambda_{fc,o}^a\right)^{1/a} \quad (43)$$

Noticeably, the receiver has chosen a cavity receiver which $a = 1$ where the amount of total convection heat loss is given by (44, 45):

$$\dot{Q}_{conv} = \lambda_{air}(T_{sur} - T_0)A_{sur} \quad (44)$$

$$\lambda_{air} = [\lambda_{air,fc} + \lambda_{air,nc}/F_r] \quad (45)$$

The conductive heat loss is assessed by Eq. (46):

$$\dot{Q}_{cond} = \frac{A_{sur}(T_{sur} - T_0)}{(\delta_{insu}/k_{insu} + 1/\lambda_{air,0})} \quad (46)$$

where \bar{T}_{ms} is the average of inlet and outlet temperature, which is written in Eqs. (47), (48):

$$\bar{T}_{ms} = \frac{T_{mi} + T_{mo}}{2} \quad (47)$$

$$\frac{\dot{Q}_{rec}}{A_{sur}} = \frac{(T_{sur} - \bar{T}_{ms})}{d_o/d_i/h_{ms} + d_o Ln(d_o/d_i)/2/k_{tube}} \quad (48)$$

In the gap of the difference of temperature between the receiving surface and the surrounding radiation, heat loss is occurred characterized by (49):

$$\dot{Q}_{em} = \epsilon\sigma(T_{sur}^4 - T_0^4) \quad (49)$$

where σ represents Stephen Boltzmann's constant. The latest type of heat loss is a reflective loss, which is caused by the reflection of the radiation from the receiving surface, which has been influenced by material manufacturing. The relation (50) determines the reflective heat loss radiation:

$$\dot{Q}_{ref} = \rho\dot{Q}_{rec}F_r \quad (50)$$

The second thermodynamics law for absorbing energy of the input exergy is given in Eq. (51):

$$\dot{\psi}_{abs} = \dot{m}_{ms}C_{pms}[(T_{mo} - T_{mi}) - T_0 Ln(T_{mo}/T_{mi})] \quad (51)$$

The energy efficiency at the center receiver is defined as the fraction of absorbing and receiving energy in Eq. (52):

$$\eta_{solar} = \dot{Q}_{abs}/\dot{Q}_{rec} \quad (52)$$

Biomass

Biomass is a renewable energy source derived from biological materials. In general, wastes that are of biological origin and have arisen from cell proliferation are called biomass. The heat produced from the biomass is calculated as follows [45].

$$\dot{Q}_{gen} = \dot{m}_{bio}(h_{bio} - h_o) \tag{53}$$

Boiler or evaporator presumed the biomass boiler efficiency of 65%, and for total combustion efficiency, it assumed 15%, and the heat transfers in the boiler are considered by the reformation of generative heat in the boiler based on reforming by two efficiencies (total combustion efficiency and biomass boiler efficiency) defined as (54):

$$\dot{Q}_{boiler} = 0.8 \times 0.9 \dot{Q}_{gen} \tag{54}$$

When the biomass source has been chosen, the environmental pollution is delivered to the surroundings by emission in gas turbine (GT) and HRSG of the plant such as faulty combustion of the gasifier/combustor section in GT, Also, NOx will be generated because the gas turbine ignition fired in high temperature. GT exhausts to the surroundings consisting of NOx, SOx, CO, CO2, unburned hydrocarbons (HC), VOCs, and particulates. In the biomass source, the production of the sulfur compounds and nitrogen compounds is converted to SOx and NOx in the gasifier/combustor of GT. The emission of material such as NOx, SOx, CO, CO2, CH4, (HC) except CH4, VOCs, and particulates is orderly, 479, 254, 0.86, 916,224, 0.27, 0.53, 515 and 3.7 in units of (Kg/GWh). [46] simulated by using the ASPEN Plus™ for each emission material was earlier discussed.

Economic modeling

Brayton cycle and organic Rankine cycle

The choice of the best heat sources for the economic analysis is the vital approximation for the combination of cycles such as coupling of three Rankine cycle, Brayton cycle, and organic Rankine cycle.

The Rankine cycle consists of turbine, pump, condenser, boiler/evaporator; initialization of the cost of the cycle was important, and some ignorable costs for example for piping and repairing for initial cost are neglected. Approximately, in the Rankine cycle, the initial cost is estimated in Eq. (55):

$$C_{RC} = b_1 w_t^{d_1} + b_2 A_{cond}^{d_2} + b_3 A_{boiler}^{d_3} + b_4 w_p^{d_4} \tag{55}$$

The amounts of *b* and amounts of *d* were identified by [47] in this study, for constant (*b*) valued [1673, 4750, 150, 3500] and, for constant (*d*) valued [0.8 0.47 0.8 0.75]. Because of using a solar collector, the cost of new modules should be supplementarily increased to the first estimation cost of the cycle.

The specific cost (SC) is used for an economic assessment of the Brayton cycle. It related to the investment cost to the operative machines parameter; for example, mass flow

rates, pressure ratio, isentropic efficiency, and turbine inlet temperature considered in Celsius degrees unit [48].

The SC represented the cost of installation of a plant per electrical kilowatt (kW) installed. SC is defined as:

$$SC = \frac{C_{BC}}{\dot{W}_{GT}} \tag{56}$$

where C_{BC} the investment cost of the Brayton cycle and $\dot{W}_{net,BC}$ is the network of the Brayton cycle.

Based on costs for the turbine and the compressor in the Brayton cycle, the C_{BC} can be intended to Eqs. (57) and (58):

$$C_{TUR} = 479.34 \dot{m}_{TUR} \left(\frac{1}{0.93 - \eta_{TUR}} \right) \ln(r_{p,TUR}) (1 + \exp(0.036T_{TUR,i} - 54.4)) \tag{57}$$

$$C_{COMP} = 71.10 \dot{m}_{COMP} \left(\frac{1}{0.92 - \eta_{COMP}} \right) r_{p,COMP} \ln(r_{p,COMP}) \tag{58}$$

where $T_{TUR,i}$ is the inlet temperature of the turbine in Celsius degree, \dot{m}_{TUR} is mass flow rates of the turbine in Brayton cycle, \dot{m}_{COMP} is mass flow rates of the compressor in Brayton cycle, η_{TUR} is turbine efficiency, η_{COMP} is the compressor efficiency, $r_{p,COMP}$ is the pressure ratio of the compressor, and $r_{p,TUR}$ is the pressure ratio of the turbine which C_{TUR} is cost of the turbine, and C_{COMP} is cost of the compressor.

For the Brayton cycle, the C_{BC} is the summation of C_{TUR} and C_{COMP} indicated in Eq. (59):

$$C_{BC} = C_{TUR} + C_{COMP} \tag{59}$$

Solar cost

The cycle equipped by a solar tower built with a tower with a high-altitude tower, the cost of the tower named C_{tower} . Based on the altitude of the tower and the cost of constructing towers, the cost of the tower of solar collectors is defined by (60) [49]:

$$C_{tower} = 250,000 + 14.77(0.6806Q_{rec} + 106.6)^{2.395} \tag{60}$$

where Q_{rec} should be considered in (MW) unit [49].

Inside of solar collector, put a receiver for receiving the radiation of the sun where the cost of it is termed as C_{rec} where approximately it is calculated in Eq. (61) [50]:

$$C_{rec} = \frac{46438}{\dot{q}_{rec}} + 21.899 \left[\frac{\text{€}}{\text{Kw}} \right] \tag{61}$$

where \dot{q}_{rec} considered the input flux receiver in (kW) unit. Heliostats as a mirror for reflecting light are placed into a

solar collector. The cost of a mirror named $C_{\text{heliostats}}$ the cost function for building a solar tower includes costs such as the cost of the tower height, the cost of the equipment inside the receiver, and consider the cost of mirrors needed to reflect

light. The cost function for a mirror of the solar tower is defined as in Eq. (62) [51]:

$$C_{\text{Heliostats}} = 140A_h \text{ [€]} \tag{62}$$

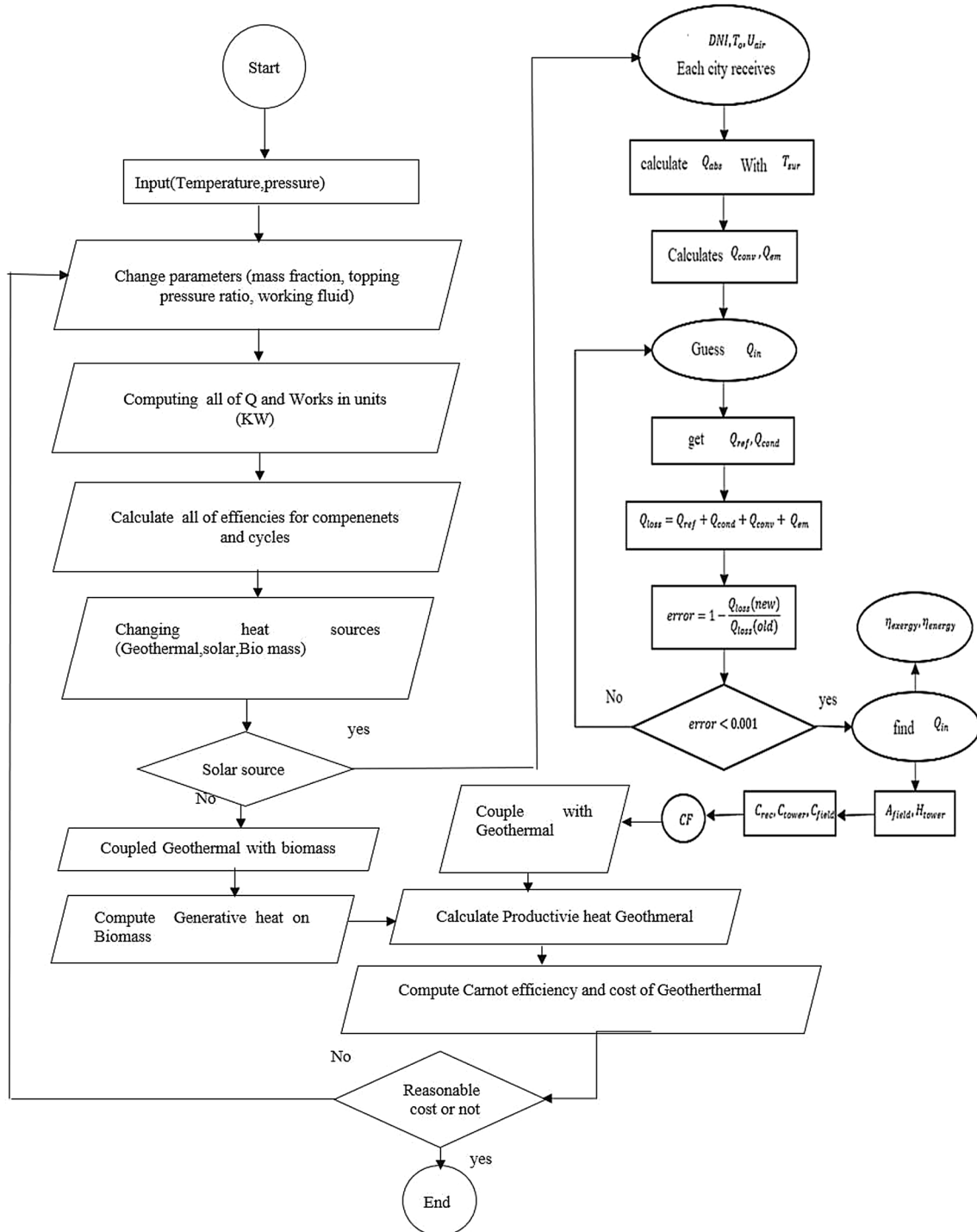


Fig. 2 Flowchart for the programming based on thermodynamics and economics equations of combination triple cycle by the variation heat source

Table 4 Enthalpy and entropy assessment validation

State No	h_{ref} (kJ/kg)	$h_{current}$ (kJ/kg)	$\frac{ h_{current}-h_{ref} \times 100}{h_{ref}}$ (%)	s_{ref} (kJ/kg k)	$s_{current}$ (kJ/kg k)	$\frac{ s_{current}-s_{ref} \times 100}{s_{ref}}$ (%)
1	300.209	298.2	0.6692	5.703	6.862	20.32264
2	793.97	618.4	22.11293	5.75	6.933	20.57391
3	1363.97	1112	18.47328	6.416	7.537	17.47195
4	638.34	684.9	7.293919	6.49	7.57	16.64099
5	668.134	664.8	0.499002	1.95	1.918	1.641026
6	3006.3	2794	7.061837	6.34	5.974	5.772871
7	2843.58	2656	6.596614	6.43	6.045	5.987558
8	3086	3086	0	6.87	6.873	0.043668
8a	2763.68	2731	1.182481	7.5	7.5	0
9	2293.68	2293	0.029647	7.52	8.709	15.81117
10	137.75	137.1	0.471869	0.476	0.4741	0.39916
11	137.87	137.1	0.558497	0.476	0.4741	0.39916
12	663.024	656	1.059388	1.914	1.359	28.99687
13	453.225	503.3	11.0486	6.08	7.36	21.05263
14	567.75	578.2	1.840599	2.087	2.268	8.672736
15	466.17	438.9	5.849797	2.164	2.033	6.053604
16	253.24	264.8	4.56484	1.18	1.217	3.135593
17	253.25	265.4	4.797631	1.18	1.218	3.220339

The cost of solar collectors defined the summation of these three costs, C_{tower} , C_{rec} and $C_{heliostats}$ in Eq. (63),

$$CF = C_{tower} + C_{rec} + C_{heliostats} \tag{63}$$

To achieve the annual investment cost, it has been defined as the annual capital recovery factor (CRF) where it has been calculated by Eq. (64):

$$CRF = \frac{i(1+i)^n}{(1+i)^n - 1} \tag{64}$$

In CRF, (i) is the annual interest rate and equipment lifetime (n) another meaning for account the life of the equipment it takes into parameters (n) and the annual profit (i) has been considered. In this study, the values of (i) and (n) are 0.137 and 25 years, correspondingly. For account, the cost of repairs took into 0.02, the cost of the equipment, at last, the cost of the collector is guessed to Eq. (65):

$$C = \frac{PEC}{CRF} + 0.02PEC \tag{65}$$

Geothermal

The fuel source of geothermal is the thermal of the core of the ground, and the cost of the first source is free but the cost of the foundation of a geothermal plant is more expensive than the other plants. Mostly, the economic analysis of the geothermal power plant is explained with the purposes of the model by the levelized cost of electricity (LCOE). LCOE is

the cost of the necessity of electricity resource production in instruction to break the lifetime of the project. From geothermal power plant station, LCOE is calculated as follows:

$$LCOE = \frac{\sum_{n=1}^t \frac{I_t+M_t+F_t}{(1+r)^t}}{\sum_{n=1}^t \frac{E_t}{(1+r)^t}} \tag{66}$$

The expense of the power system and improper power system can be led with an LCOE of 128 €/MWh which the effects of source greenhouse gas (GHG) emission anticipated for 2050 may be zero. GHG can be led with LCOE of 54 €/MWh prices [52].

In LCOE, the parameter noticed n is the time life of the system, r is the rate of discounting, I_t is investment cost including financing expenses per year, M_t is set-ups, and preservation costs per t year. F_t is fuel payments per t year, and E_t is electricity generation per t year.

Biomass

Biomass is considered a renewable energy source. Biomaterials use as a source of energy, commonly, the waste of biomaterials can be renewed. Biologically, the most dangerous waste of biomass is the waste of radioactive nuclear cells. The heat has been released by biomass fuel such as wheat waste, waste of tomatoes, and potato waste, orderly, 17,000 (kJ/kg), 16,000 (kJ/kg), and 25,000 (kJ/kg). Cost of biomass fuel for each material such as waste wheat is 30 (\$/Ton), waste tomatoes are 60 (\$/Ton), waste potato is 20 (\$/

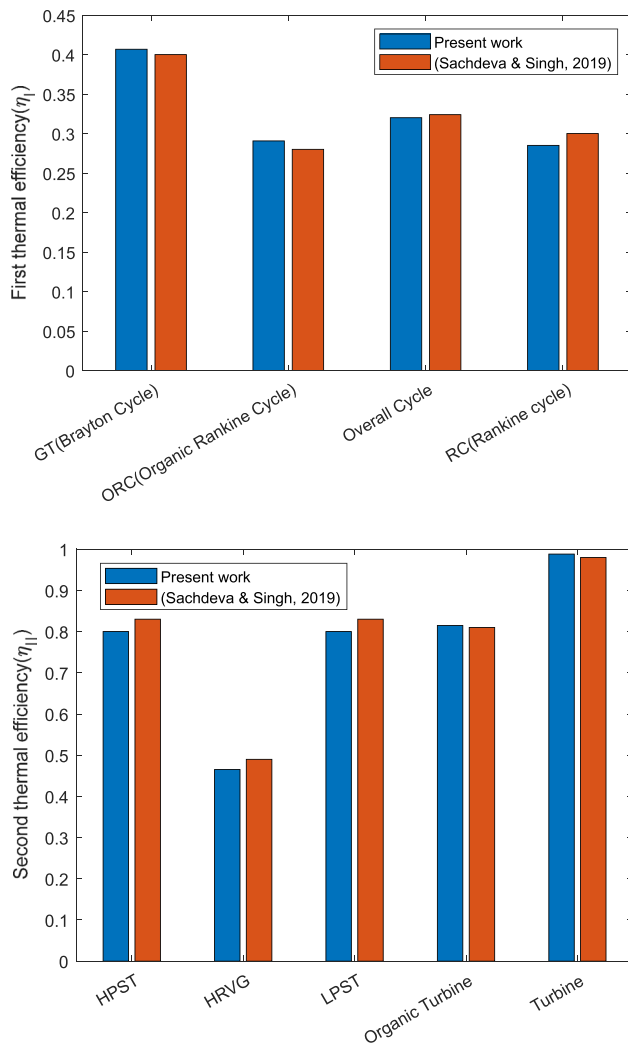


Fig. 3 Validation of the same power plant: **a** first thermal efficiency, **b** second thermal efficiency with Ref. [38]

Ton) which has been assumed [44]. The flowchart of this case is shown in Fig. 2

Genetic algorithm

Genetic algorithm [53] is a computer science search technique for finding approximate solutions to optimization and search problems. Genetic algorithms are a special type of evolutionary algorithm that uses biological techniques such as inheritance and mutation.

Genetic algorithms are usually implemented as a computer simulator in which the population of an abstract sample (chromosomes) of the solution candidates of an optimization problem leads to a better solution. Traditionally, solutions were in the form of strings of 0 and 1, but today they are implemented in other ways as well. The hypothesis

begins with a unique random population and continues through generations. In each generation, the capacity of the entire population is assessed, several individuals are randomly selected from the current generation (based on competencies) and modified to form a new generation (deducted or recombined), and then the algorithm is converted to the current generation.

Results and discussion

Thermodynamics analysis

Validation

In this study, the effect of using different energy sources on the performance of the triple combined cycle consisting of the Rankine cycle, Brayton cycle (BC), and organic Rankine cycle is investigated. The proposed thermodynamic and economic modeling of the proposed cycle has been performed, and the results of this modeling have been compared with the previous literature to examine the accuracy of modeling. The validation of this study with [38] at conditions of pressure ratio (r_p) of BC, high pressure, and low pressure is 24, 50 bar and 20 bar, respectively.

The assessment validation for entropy and enthalpy is given in Table 4. The presented table shows the good precision for assessment.

Figure 3 shows the validation results of this paper. The percentage difference between the results of the two studies is about 0.5%, which indicates a good match between the results, and the present modeling has good accuracy.

GT (Brayton cycle)

According to the first and second laws, the effect of heat sources on the performance of the combined cycle has been investigated to select the appropriate heat source. The effect of using different organic fluids has also been investigated.

The parameters which have effects on the Brayton cycle which improved the performance of the combined cycle consist of changing fluid, r_p and m_a . The effect of using different fluids in a Brayton cycle such as air, CO, CO₂, N₂, and NO₂ on the thermal efficiency of the turbine and compressor and the Brayton cycle and the overall thermal efficiency is shown in Fig. 4. The mass flow rate of the working fluid mass in the Brayton cycle is considered to be equal to 10 kg/s. The highest and lowest total thermal efficiency (I) with values of 32.98% and 30.64% belong to CO and NO₂. Besides, the changing of working fluid in GT affects the efficiency of the second law as well as



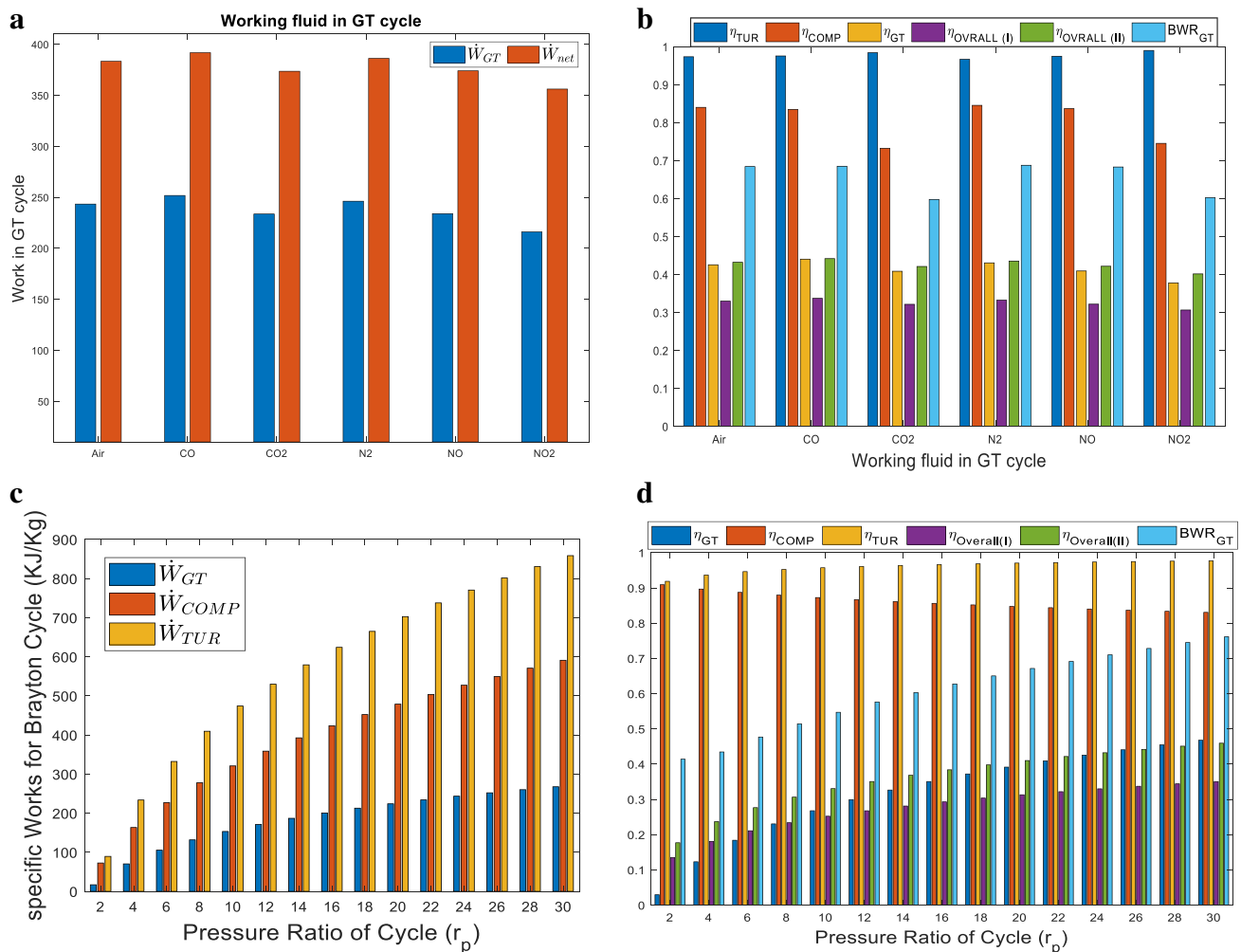


Fig. 4 Effects of changing working fluid, **a** effect on specific network and specific work of GT, **b** effects on $\eta_{overall(I)}$, $\eta_{overall(II)}$, η_{GT} , effects of varying (r_p), **c** effect on specific network and specific work of GT and **d**)effects on the thermal efficiencies

the efficiency of the first law, and the high thermal efficiency (II) belongs to CO and NO2, orderly, they have been valued as 43.21% and 40.14%, respectively. Changes in the thermal efficiency of the Brayton and turbine cycles are the same factor in terms of fluid change, and N2 has maximum efficiency in GT because of being the highest value of \dot{W}_{GT} as shown in Fig. 4a. Changes in compressor and BWR efficiency are similar to changing the type of operating fluid in the Brayton cycle. When N₂ is used, the highest efficiency of the compressor and BWR is achieved. Thus, changing the working fluid in GT has effects on the specific work and efficiency of the turbine and compressor. The BWR depends on changing the generative and combustion-specific works also, thermal efficiency be reliant on the changing of net output power, which is shown in Fig. 4c. The overall thermal efficiency of the combined cycle in terms of (r_p) is shown in Fig. 4d. The overall thermal efficiency of the cycle increases as the pressure ratio

increases as a curve. The slope of the efficiency changes is high in the low-pressure ratio and low in the high-pressure ratio. The changes in efficiency and specific work in terms of variation pressure ratio of GT (r_p) are shown in Fig. 4d. By increasing the pressure ratio, the thermal efficiency of the Brayton cycle, turbine, and compressor in this cycle increases by about 33.26%, 0.44%, and 0.64%, respectively. The back-work ratio (BWR) for the GT cycle is defined as friction W_{COMP} and W_{TUR} , and BWR has been increased with changes (r_p) shown in Fig. 4d which consequences necessity of more generative power in the turbine for combustion in the compressor. One of the important variables in the logical design of a cycle that affects the efficiency of the power cycle and its output power is the mass flow rate of the operating fluid in that cycle. The effect of changing the airflow rate in the Brayton cycle on the thermal efficiency and power of the Brayton cycle, BWR, and total thermal efficiency (I) and total thermal

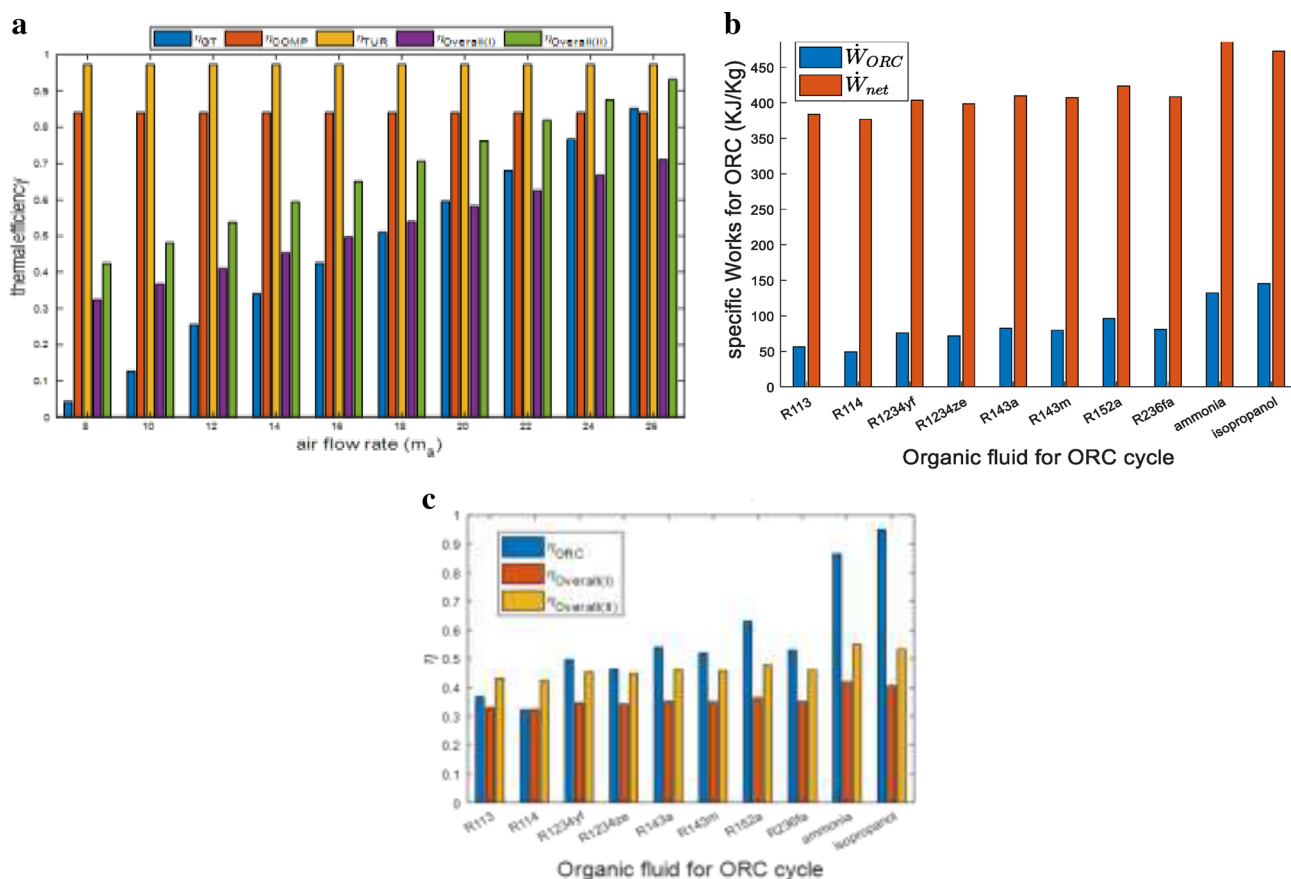


Fig. 5 Effects of varying (m_a): **a** effects on the thermal efficiencies changing organic fluid in ORC effects on **b** specific work, and **c** thermal efficiencies

efficiency (II) of the cycle has been investigated, and the results are shown in Fig. 4.

The power of the compressor, turbine, and Brayton cycle changes linearly with the air mass flow rate and increases with increasing air mass flow rate. The thermal efficiency of the Brayton cycle increases with increasing air mass flow rate. Because it increases the output power of the gas turbine, the thermal efficiency of the turbine and compressor of this cycle does not change much. BWR is independent of air mass flow rate, and changing the air mass flow rate does not have a significant effect on it. Rising air mass flow rate has a linear increasing effect on the overall thermal efficiency of the cycle because of increasing the network in overall thermal efficiency rather the increasing the inlet heat as shown in Fig. 4.

ORC (organic Rankine cycle)

The overall efficiency of the cycle and the efficiency of the organic Rankine cycle and their output power have been investigated. According to the change in the type of organic fluid and its results shown in Fig. 5, the Rankine organic

cycle (ORC) is named for the use of an organic fluid with a high molecular weight, which changes its liquid–vapor phase or boiling point at a temperature below the water–vapor phase change temperature. The fluid allows the Rankine cycle to recover heat from low-temperature sources such as biomass combustion, industrial heat loss, geothermal, solar, and low-temperature heat, which can be converted into electricity. Different types of organic fluids such as R113, R114, R1234yf, R1234ze, R143a, R143m, R152m, R236fa, ammonia, and isopropanol are considered. Fluids ammonia and isopropanol have the highest and lowest combined power output cycles with organic Rankine cycle efficiency of 0.8654 and 0.9499, and amount of the thermal overall efficiency equal to 0.4196 and 0.4067, respectively. The reason for the difference in the results indicates that parameters such as latent heat, density, specific heat, and, most importantly, the type of working fluid have a great impact on the output and output values.



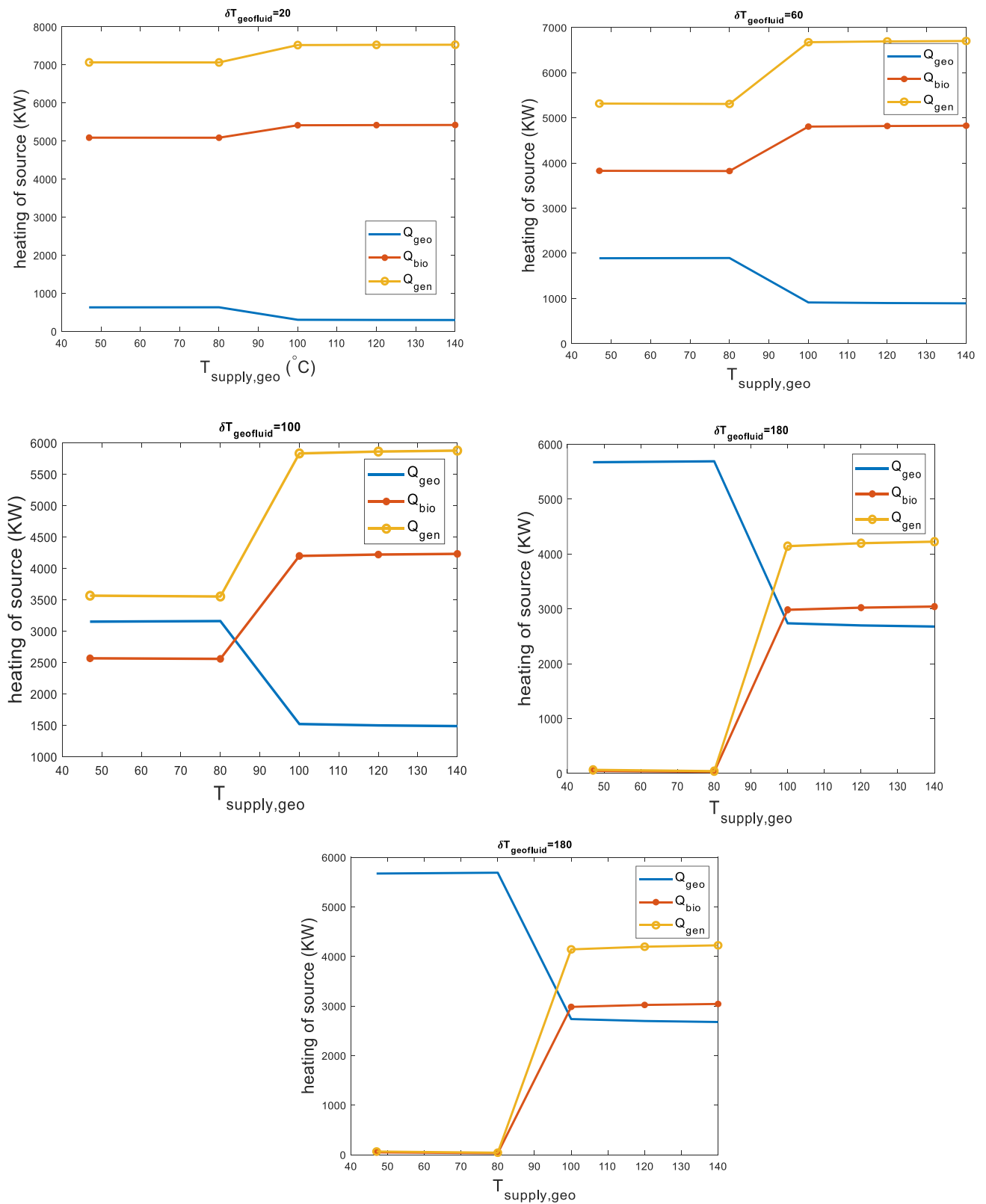


Fig. 6 Changing geothermal parameters based on coupling with biomass

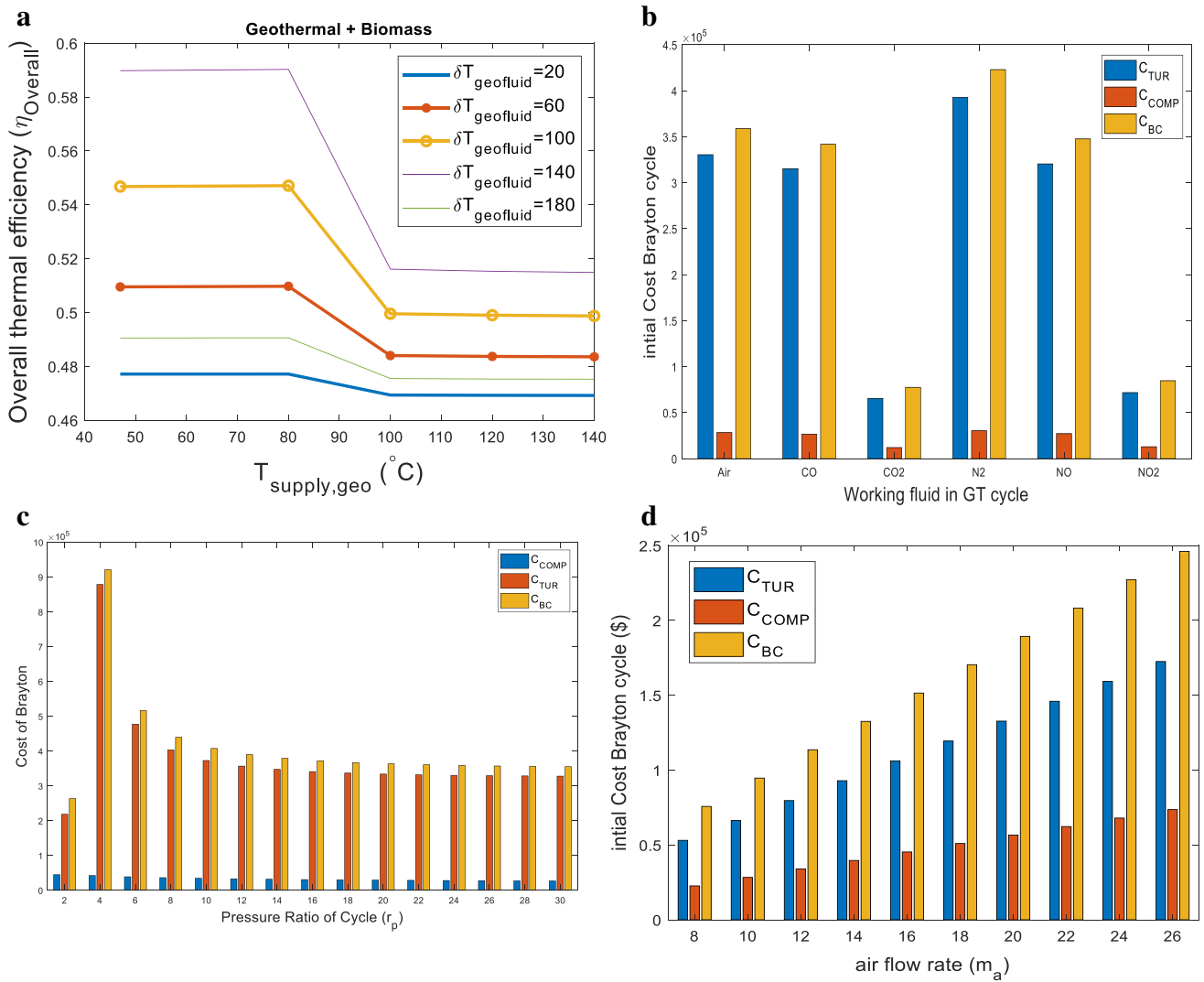


Fig. 7 a Thermal efficiency coupling of geothermal and biomass by alternative geothermal parameters, the initial cost for cycles by changing, b working fluid and c pressure ratio in GT cycle and d initial cost for cycles changes in terms of air mass flow

Table 5 Characteristics of the designed solar tower

η_{solar}	$T_{surface}(k)$	$H_{solar\ tower}(m)$	$\dot{Q}_{abs\ solar}(kW)$	
0.728	505.68	107.9	1418kw	Summer
0.8835	22.22	110.8	5569.3	Winter

Geothermal

Inlet heat due to geothermal depends on the temperature design of the geothermal station. $\delta T_{geofluid} = 20\text{--}180$ is different temperatures relate to the design temperature of geothermal from the difference of supply temperature and return temperature, which is optional. Geothermal supplied the inlet temperature. The amount of $T_{supply\ geo} = 45\text{--}140$ $^{\circ}C$ has been chosen which depends on the thermophysical

of geofluid. Water has been used as the working fluid. In amount of $T_{supply\ geo} = 45\text{--}80$ $^{\circ}C$, the inlet, the heat of geothermal, is constant but at the start of the point, $T_{supply\ geo} = 80$ $^{\circ}C$ because of phase changing of geofluid in geothermal power section changing heat capacity rate. It has been decreased to reach the boiling point of water in $T_{supply\ geo} = 100$ $^{\circ}C$, and after that the geofluid changed to the vapor and the heat capacity rate is constant to the end of chosen temperature. Biomass relieves the lack of necessity of heat source to the absorber by the amount of Q_{bio} and recovers of wasting and necessity of inlet heating and generate more than the inlet of absorber with Q_{gen} which lost heat in the path of the entrancing absorber.

By increasing the $\delta T_{geofluid}$, the difference between starting the phase change and ending the phase change 100 increases, and the necessity of biomass relief has been

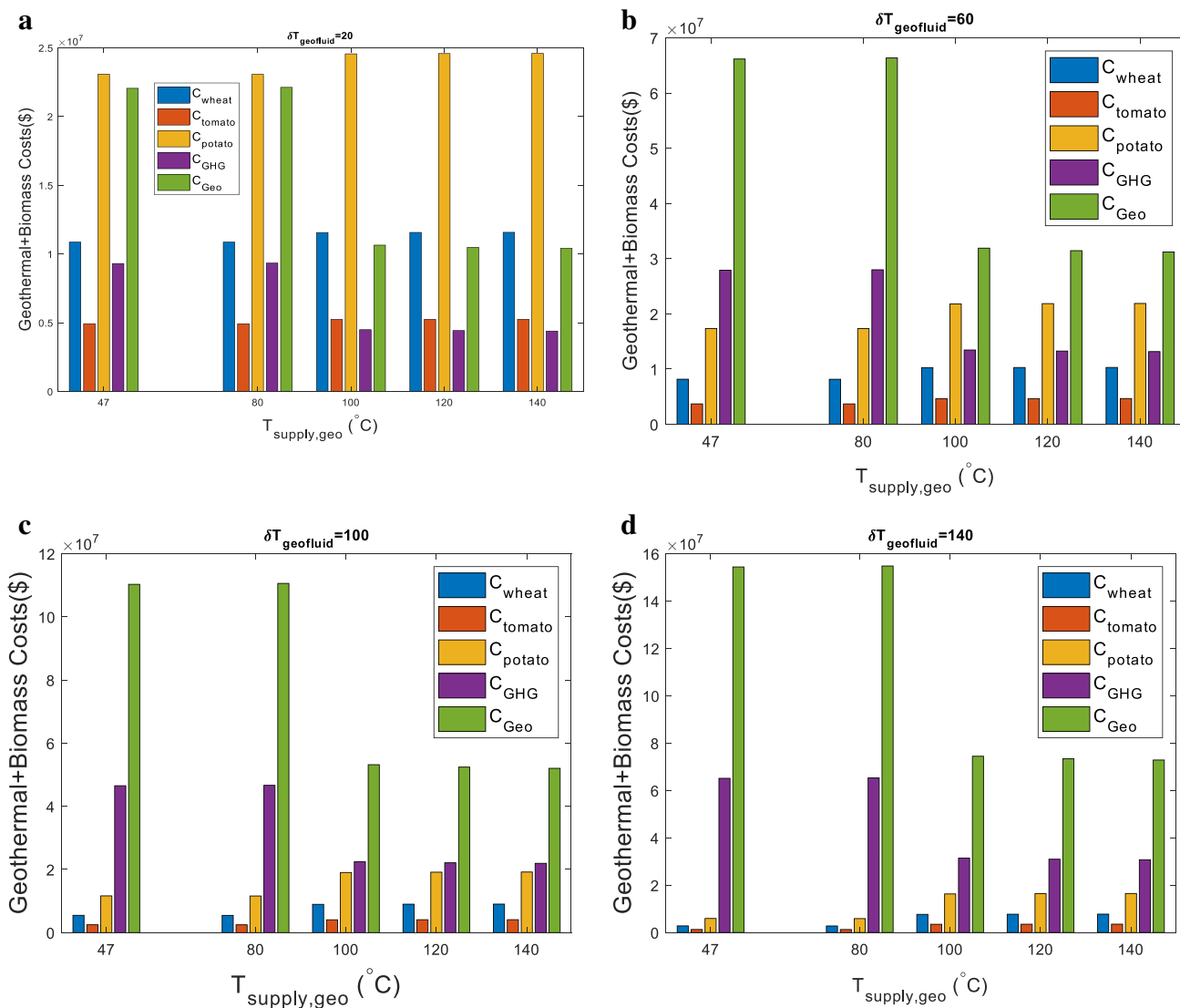


Fig. 8 Cost of geothermal–biomass by changing parameters of geothermal and different biomass fuel at **a** $\delta T_{\text{geofluid}} = 20$ and **b** $\delta T_{\text{geofluid}} = 60$

decreased as shown in Fig. 6. The changing of the heat of biomass and geothermal, the total thermal efficiency changed as shown in Fig. 7a where the network is considered as a constant value for comparison of just geothermal parameters in the situation of coupling geothermal with biomass. At the point of starting phase change, increase in generative heat in biomass recovered is more than the decrease in generative heat by geothermal, and total generate heat will be increased because of the decrease in the total efficiency until the boiling point. Also, by changing of $\delta T_{\text{geofluid}} = 20\text{--}140$, the overall efficiency has been increased, after all, $\delta T_{\text{geofluid}} = 180$ decreased rather than $\delta T_{\text{geofluid}} = 140$ because of reducing generative biomass inlet heat source recovery.

Using the solar tower, part of the heat required for the combined cycle can be provided. Due to the average intensity of sunlight in winter and summer, the solar tower is designed to provide cycle heat. In this case, the cycle uses the geothermal–solar heat source. The results of the solar tower design are given in Table 5. According to the heat required in summer and winter, the share of heat required by the sun is higher in winter than in summer.

Economics analysis

According to the proposed modeling, the initial cost of the cycle and the cost of heat sources are investigated.

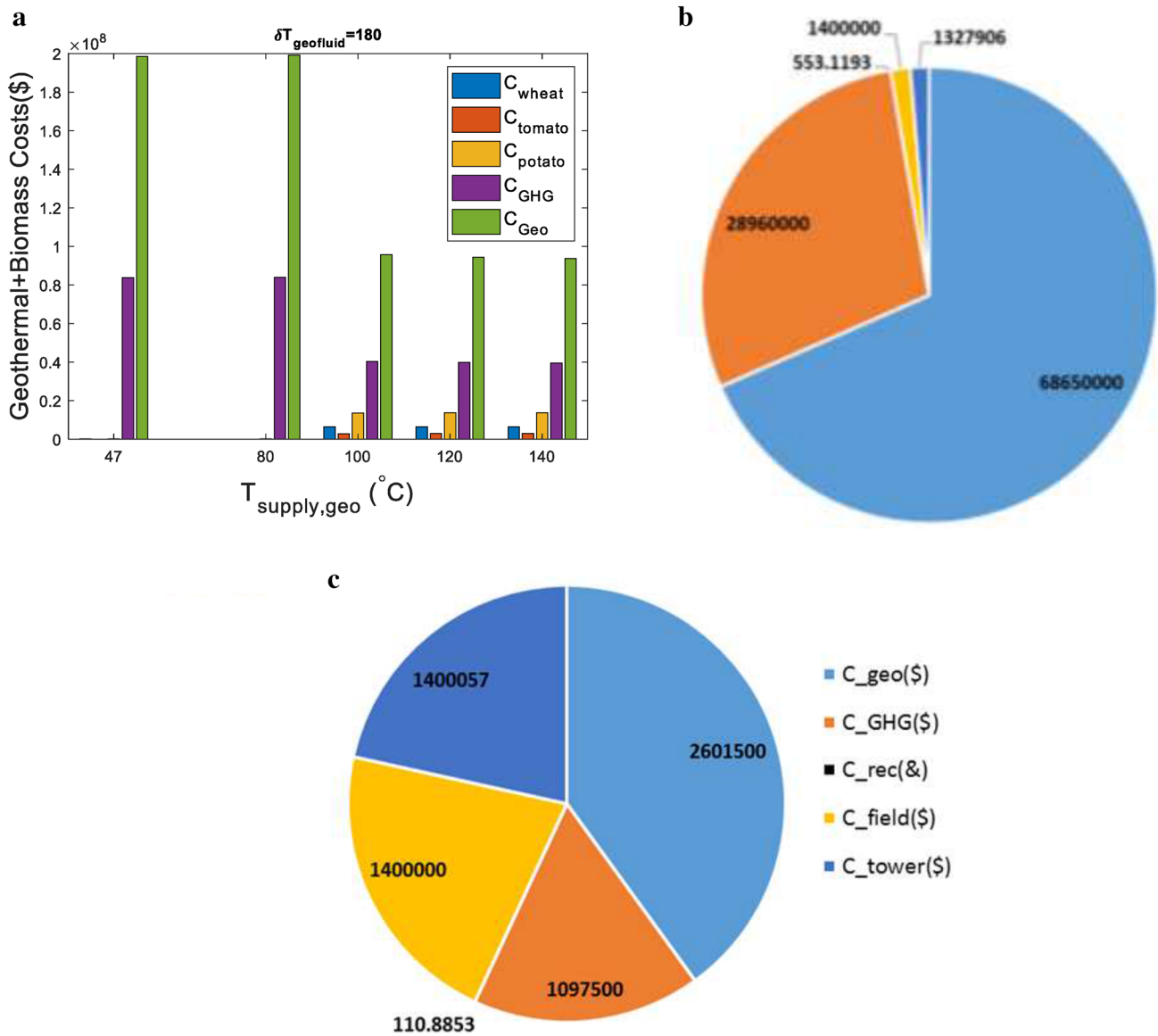


Fig. 9 a Cost of geothermal–biomass by changing parameters of geothermal and different biomass fuel at $\delta T_{\text{geo fluid}} = 180$, solar costs specifications designed for **b** summer and **c** winter

Initialization cycle cost

First, the economical modeling of the initialization cost of two Rankine cycles (steam reheat cycle and ORC) and the Brayton cycle for estimation of the total cycle must be considered. According to the equation cost for the Rankine cycle, the cost of two Rankine cycles has been initialized as 1.31×10^6 \$. Thermodynamically, some parameters have effects on the performance of the total cycle, also they affect the initialization cost of the Brayton cycle, such as changing fluid, the pressure ratio of the cycle, and airflow rate. Based on the economic modeling, changing the airflow rate in the Brayton cycle and the pressure-to-fluid ratio in the Brayton

cycle and the organic Rankin cycle affect the cost of the cycles and change it. These changes are shown in Fig. 7b–d. As the pressure ratio increases, the cost of the Brayton cycle increases so that it reaches its maximum value at $r_p = 4$ and then decreases. By increasing the mass flow rate of the Brayton cycle, the cost of this cycle also increased.

Heat source cost

The heat received from the geothermal source is not sufficient as the heat entering the gas turbine cycle, and biomass or solar energy is used to supply some of the heat required by the cycle. Both energy supply states, geothermal–biomass

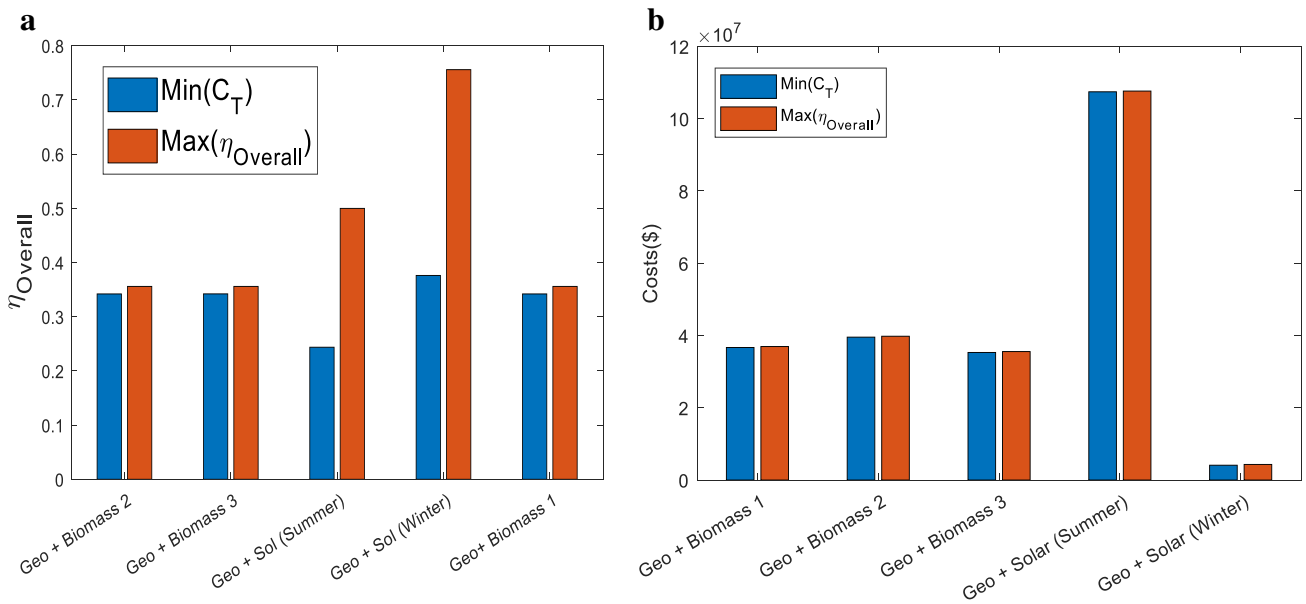


Fig. 10 a Optimal of $\eta_{overall}$ for each heat source, b optimal of C_{Total} for each heat source

Table 6 Minimization of C_{Total} for each heat source

m_a	$T_{geo, supply}$	$\delta_{geofluid}$	r_p	m_r	Biomass	Heat source
8	341.1	144.9	19.08	0.1	–	Geothermal + solar (summer)
8	353.3	53.2	19.04	0.1	–	Geothermal + solar (winter)
8	293	20	29.97	0.1	Wheat	Geothermal + biomass 1
8	293	20	29.94	0.1	Potato	Geothermal + biomass 2
8	293	20	30	0.1	Tomato	Geothermal + biomass 3

Table 7 Maximization of $\eta_{overall}$ for each heat source

m_a	$T_{geo, supply}$	$\delta_{geofluid}$	r_p	m_r	Biomass	Heat source
26	413	180	30	1	–	Geothermal + solar (summer)
26	293	20	30	0.1	–	Geothermal + solar (winter)
8	303.6	20.08	30	0.9992	Wheat	Geothermal + biomass 1
8	303.6	20.08	30	0.9992	Potato	Geothermal + biomass 2
8	303.6	20.08	30	0.9992	Tomato	Geothermal + biomass 3

Table 8 Emission of material (HC, NOX, particulate, SOX, and VOCs) for geothermal/ biomass in units of megatons

Source	HC	NOX	Particulate	SOX	VOCs
Biomass	8.030E-07	0.0007257	0.000005606	0.0003848	0.0007802
Geothermal	–	–	–	–	–
Geothermal + biomass	8.030E-07	0.0007257	0.000005606	0.0003848	0.0007802

and geothermal–solar, are estimated for the cycle, and the cost of the triple cycle is estimated. Figure 6 provides the required heat supply for the combined cycle through geothermal–biomass. The heat received through geothermal depends on $\delta T_{geofluid}$ and $T_{supply geo}$, so that when $T_{supply geo}$ rises above 80 °C, the amount of heat received in $\delta T_{geofluid}$

= 20 and 60 °C increases and decreases for $\delta T_{geofluid} = 100$ and 180 °C and different biomass fuel at (a) $\delta T_{geofluid} = 20$ and (b) $\delta T_{geofluid} = 60$. The cost of using biomass energy is calculated according to the type of biomass material, and the difference between geothermal fluid temperature and geothermal fluid input temperature is shown in Figs. 8 and 9a.

Table 9 Emission of material for geothermal/biomass cycle in units of megatons

Source	CH ₄	CO	NO ₂	CO ₂
Biomass	4.091E-07	0.000001303	Convert to NOX	1.388
Geothermal	6.868E-07	–	6.868E-07	0.03605
Coupling Geothermal + biomass	0.000001096	0.000001303	6.868E-07	1.424

Table 10 Emission of material for geothermal/solar cycle in units of megatons

Source	CH ₄	NO ₂	CO ₂
Geothermal + solar(summer)	1.6185e-06	1.6185e-06	0.0849
Geothermal + solar(winter)	6.1350e-08	6.1350e-08	0.0032
Total Geothermal + solar	1.6799e-06	1.6799e-06	0.0882

Costs for different parts of the solar tower and geothermal are shown in Fig. 9b, c. The cost of geothermal is much higher in summer than in winter. The cost of a solar tower is relatively 74% higher in summer than in winter. In addition, the highest cost of a solar tower is related to mirrors.

The effect of variables such as m_a , $T_{\text{geo, supply}}$, δ_{geofluid} , r_p and m_r on the performance of the triple cycle was investigated, and it was observed that they have different effects on the efficiency of the proposed cycle. Therefore, the optimal values of these variables are determined to achieve better performance of the cycle, the highest efficiency, and the lowest cost, using the genetic algorithm (GA).

Cycle cost (C_{Total}) and efficiency (η_{overall}) have been selected as the objective function for optimization. The bounds of effective parameters have been selected as $8 \leq m_a \leq 26$, $290 \leq T_{\text{geo, supply}} \leq 413$, $20 \leq \delta_{\text{geofluid}} \leq 180$, $2 \leq r_p \leq 30$ and $0.1 \leq m_r \leq 1$; for this case, selection parameters of each heat source for maximization of η_{overall} or minimization of C_{Total} have been calculated by a genetic algorithm. Figure 10 a&b illustrates η_{overall} and C_{Total} in this optimization. From Fig. 10, it can be seen that using the geothermal and biomass system with three biofuels has been considered, and it has been indicated Geo + Biomass 1, Geo + Biomass 2, and Geo + Biomass 3, orderly, the biofuels were wheat, potato, and tomato. A cycle with high efficiency and lower cost compared to the geothermal can be known that the coupling of geothermal with solar was more efficient than the coupling geothermal with biomass. When tomatoes waste is used as biomass fuel, the cost of the proposed cycle is lower. Although the coupling of geothermal with the solar system was more expensive,

eventually the solar system can be achieved. The optimal values of design variables are given in Tables 6 and 7.

Consequently, the environmental effects of the proposed cycle in the optimal state are studied and presented in Table 8. Therefore, biomass has destructive environmental effects. Also, destructive emission material for the environment such as CO₂, CH₄, and SO₂ has been emitted by a geothermal source. It is given in Table 9. Estimation of this triple combination cycle with a heat source of coupling geothermal with biomass for the next 30 years (2020–2050) in units of Megatons for CH₄, NO₂, and CO₂ is given in Tables 9 and 10. It can be found that geothermal–solar composition has less destructive environmental effects than geothermal–biomass composition but the cost is high.

Conclusions

In this study, the thermodynamic and economic analysis for a triple combination of a Rankine cycle, an organic Rankine cycle (ORC), and Brayton with different energy sources and coupling the sources for the necessity of provision of heating, the inlet of the gas turbine in the Brayton is investigated. Biomass, geothermal and solar energy are considered sources of energy supply.

The effect of changing the working fluid of the gas turbine cycle has been investigated, and the highest and lowest total thermal efficiency (η) belong to CO and NO₂ with values of 32.98% and 30.64%, respectively. It is observed that thermal efficiency of the Brayton cycle, the turbine, and the compressor in this cycle were increased almost 33.26%, 0.44%, and 0.64% by increasing the pressure ratio, respectively. The effect of the organic fluid change on the organic Rankine cycle has been investigated, and ammonia and isopropanol have the highest and lowest combined power output cycles with organic Rankine cycle efficiency 0.8654 and 0.9499, amount of the overall thermal efficiency equal to 0.4196 and 0.4067, respectively. In the geothermal case, as the temperature increases, the heat input of the cycle increases except in the range of 80–100 °C. In this range, a decrease in supply heat has been observed. Such behavior has also been observed for overall thermal efficiency. The total thermal efficiency increases by increasing the $\delta T_{\text{geofluid}}$.

The two objective functions of thermal efficiency and cost of the proposed cycle are considered as objective functions and the optimal states are determined using the genetic algorithm. It can be seen that using the geothermal and biomass system, a cycle with high efficiency and lower cost compared to the geothermal and solar system can be achieved. The environmental analysis states that geothermal–solar composition has less destructive environmental effects than geothermal–biomass composition.



References

- Evans, A., Strezov, V., Evans, T.J.: Assessment of utility energy storage options for increased renewable energy penetration. *Renew. Sustain. Energy Rev.* **16**(6), 4141–4147 (2012). <https://doi.org/10.1016/j.rser.2012.03.048>
- Karkour, S., Ichisugi, Y., Abeynayaka, A., Itsubo, N.: External-cost estimation of electricity generation in G20 countries: case study using a global life-cycle impact-assessment method. *Sustainability* **12**(5), 2002 (2020)
- Chen, H., Cong, T.N., Yang, W., Tan, C., Li, Y., Ding, Y.: Progress in electrical energy storage system: a critical review. *Prog. Nat. Sci.* **19**(3), 291–312 (2009)
- Menéndez, J., Ordóñez, A., Álvarez, R., Loredó, J.: Energy from closed mines: underground energy storage and geothermal applications. *Renew. Sustain. Energy Rev.* **108**, 498–512 (2019). <https://doi.org/10.1016/j.rser.2019.04.007>
- Burer, M., Tanaka, K., Favrat, D., Yamada, K.: Multi-criteria optimization of a district cogeneration plant integrating a solid oxide fuel cell–gas turbine combined cycle, heat pumps and chillers. *Energy* **28**(6), 497–518 (2003). [https://doi.org/10.1016/S0360-5442\(02\)00161-5](https://doi.org/10.1016/S0360-5442(02)00161-5)
- Al-Sulaiman, F.A., Hamdullahpur, F., Dincer, I.: Trigenation: a comprehensive review based on prime movers. *Int. J. Energy Res.* **35**(3), 233–258 (2011). <https://doi.org/10.1002/er.1687>
- Wang, H., Peterson, R., Herron, T.: Design study of configurations on system COP for a combined ORC (organic Rankine cycle) and VCC (vapor compression cycle). *Energy* **36**(8), 4809–4820 (2011). <https://doi.org/10.1016/j.energy.2011.05.015>
- Carvalho, M., Serra, L.M., Lozano, M.A.: Optimal synthesis of trigenation systems subject to environmental constraints. *Energy* **36**(6), 3779–3790 (2011). <https://doi.org/10.1016/j.energy.2010.09.023>
- Wu, C., Wang, S.-s., Li, J.: Exergoeconomic analysis and optimization of a combined supercritical carbon dioxide recompression Brayton/organic flash cycle for nuclear power plants. *Energy Convers. Manag.* **171**, 936–52 (2018). <https://doi.org/10.1016/j.enconman.2018.06.041>
- Khan, Y., Mishra, R.S.: Parametric (exergy-energy) analysis of parabolic trough solar collector-driven combined partial heating supercritical CO₂ cycle and organic Rankine cycle. *Energy Sources Part A Recov. Util. Environ. Effects* (2020). <https://doi.org/10.1080/15567036.2020.1788676>
- Habibi, H., Zoghi, M., Chitsaz, A., Shamsaiee, M.: Thermo-economic performance evaluation and multi-objective optimization of a screw expander-based cascade Rankine cycle integrated with parabolic trough solar collector. *Appl. Therm. Eng.* **180**, 115827 (2020). <https://doi.org/10.1016/j.applthermaleng.2020.115827>
- Tempesti, D., Fiaschi, D.: Thermo-economic assessment of a micro CHP system fuelled by geothermal and solar energy. *Energy* **58**, 45–51 (2013). <https://doi.org/10.1016/j.energy.2013.01.058>
- Mohammadkhani, F., Shokati, N., Mahmoudi, S., Yari, M., Rosen, M.: Exergoeconomic assessment and parametric study of a gas turbine-modular helium reactor combined with two organic rankine cycles. *Energy* **65**, 533–543 (2014). <https://doi.org/10.1016/j.energy.2013.11.002>
- Liu, B.-T., Chien, K.-H., Wang, C.-C.: Effect of working fluids on organic Rankine cycle for waste heat recovery. *Energy* **29**(8), 1207–1217 (2004). <https://doi.org/10.1016/j.energy.2004.01.004>
- Mikielewicz, D., Mikielewicz, J.: A thermodynamic criterion for selection of working fluid for subcritical and supercritical domestic micro CHP. *Appl. Therm. Eng.* **30**(16), 2357–2362 (2010). <https://doi.org/10.1016/j.applthermaleng.2010.05.035>
- Dai, Y., Wang, J., Gao, L.: Parametric optimization and comparative study of organic Rankine cycle (ORC) for low grade waste heat recovery. *Energy Convers. Manag.* **50**(3), 576–582 (2009). <https://doi.org/10.1016/j.enconman.2008.10.018>
- Sirignano, W., Liu, F.: Performance increases for gas-turbine engines through combustion inside the turbine. *J. Propul. Power* **15**(1), 111–118 (1999). <https://doi.org/10.2514/2.5398>
- Abd El-Maksoud, R.M.: Gas turbine with heating during the expansion in the stator blades. *Energy Convers. Manag.* **78**, 219–224 (2014). <https://doi.org/10.1016/j.enconman.2013.10.054>
- Boehm, R.F., Yang, H., Yan, J.: *Handbook of Clean Energy Systems*. Wiley (2015)
- Farahani, S.D., Alibeigi, M.: Investigation of power generated from a PVT-TEG system in Iranian cities. *J. Solar Energy Res.* **5**(4), 603–16 (2020). <https://doi.org/10.22059/jser.2020.308162.1170>
- Farahani, S.D., Sarlak, M.A., Alibeigi, M.: Thermal analysis of PVT-HEX system: electricity efficiency and air conditioning system. *J. Solar Energy Res.* **6**(1), 625–33 (2021). <https://doi.org/10.22059/jser.2020.310682.1174>
- Reyes-Belmonte, M.A., Sebastián, A., González-Aguilar, J., Romero, M.: Performance comparison of different thermodynamic cycles for an innovative central receiver solar power plant. In: AIP conference proceedings, AIP Publishing LLC (2017)
- Blanco, M., Santigosa, L.R.: *Advances in Concentrating Solar Thermal Research and Technology*. Woodhead Publishing (2016)
- Neises, T., Turchi, C.: A comparison of supercritical carbon dioxide power cycle configurations with an emphasis on CSP applications. *Energy Procedia*. **49**, 1187–1196 (2014). <https://doi.org/10.1016/j.egypro.2014.03.128>
- Turchi, C.S., Ma, Z., Neises, T.W., Wagner, M.J.: Thermodynamic study of advanced supercritical carbon dioxide power cycles for concentrating solar power systems. *J. Solar Energy Eng.* (2013). <https://doi.org/10.1115/1.4024030>
- Stein, W., Buck, R.: Advanced power cycles for concentrated solar power. *Sol. Energy* **152**, 91–105 (2017). <https://doi.org/10.1016/j.solener.2017.04.054>
- Pramanik, S., Ravikrishna, R.: A review of concentrated solar power hybrid technologies. *Appl. Therm. Eng.* **127**, 602–637 (2017). <https://doi.org/10.1016/j.applthermaleng.2017.08.038>
- Detwiler, R.L., Roberts, J.J., Ralph, W., Bonner, B.P.: *Modeling fluid flow and electrical resistivity in fractured geothermal reservoir rocks*: Lawrence Livermore National Lab (LLNL), Livermore, CA (United States) (2003)
- Fact sheets on geothermal electricity. *European Geothermal Energy Council (EGEC)*. **12** (2014)
- Lentz, Á., Almanza, R.: Parabolic troughs to increase the geothermal wells flow enthalpy. *Sol. Energy* **80**(10), 1290–1295 (2006). <https://doi.org/10.1016/j.solener.2006.04.010>
- Boyaghchi, F.A., Heidarnejad, P.: Thermo-economic assessment and multi objective optimization of a solar micro CCHP based on Organic Rankine Cycle for domestic application. *Energy Convers. Manag.* **97**, 224–234 (2015). <https://doi.org/10.1016/j.enconman.2015.03.036>
- Chen, L., Feng, H., Ge, Y.: Power and efficiency optimization for open combined regenerative Brayton and inverse Brayton cycles with regeneration before the inverse cycle. *Entropy* **22**(6), 677 (2020). <https://doi.org/10.3390/e22060677>
- Mohammadi, K., Ellingwood, K., Powell, K.: A novel triple power cycle featuring a gas turbine cycle with supercritical carbon dioxide and organic Rankine cycles: thermoeconomic analysis and optimization. *Energy Convers. Manag.* **220**, 113123 (2020). <https://doi.org/10.1016/j.enconman.2020.113123>
- Bademlioglu, A.H., Canbolat, A.S., Kaynakli, O.: Multi-objective optimization of parameters affecting organic rankine cycle performance characteristics with Taguchi-Grey relational analysis.



- Renew. Sustain. Energy Rev. **117**, 109483 (2020). <https://doi.org/10.1016/j.rser.2019.109483>
35. Rabbani, M., Ratlamwala, T., Dincer, I.: Transient energy and exergy analyses of a solar based integrated system. *J. Solar Energy Eng.* **137**(1), 011010 (2015)
36. Shahin, M.S., Orhan, M.F., Uygul, F.: Thermodynamic analysis of parabolic trough and heliostat field solar collectors integrated with a Rankine cycle for cogeneration of electricity and heat. *Sol. Energy* **136**, 183–196 (2016)
37. Shaaban, S.: Analysis of an integrated solar combined cycle with steam and organic rankine cycles as bottoming cycles. *Energy Convers. Manag.* **126**, 1003–1012 (2016)
38. Sachdeva, J., Singh, O.: Thermodynamic analysis of solar powered triple combined brayton, rankine and organic rankine cycle for carbon free power. *Renew. Energy* **139**, 765–80 (2019). <https://doi.org/10.1016/j.renene.2019.02.128>
39. Bhatt, B., Thakore, S.B.: *Stoichiometry*. Tata McGraw-Hill Education (2010)
40. Kazemi, H., Ehyaei, M.: Energy, exergy, and economic analysis of a geothermal power plant. *Adv. Geo-Energy Res.* **2**(2), 190–209 (2018). <https://doi.org/10.26804/ager.2018.02.07>
41. Noorollahi, Y., Ghasemi, G., Kowsary, F., Roumi, S., Jalilinasrabady, S.: Modelling of heat supply for natural gas pressure reduction station using geothermal energy. *Int. J. Sustain. Energy* **38**(8), 773–793 (2019). <https://doi.org/10.1080/14786451.2019.1585434>
42. Li, X., Kong, W., Wang, Z., Chang, C., Bai, F.: Thermal model and thermodynamic performance of molten salt cavity receiver. *Renew. Energy* **35**(5), 981–988 (2010)
43. Benammar, S., Khellaf, A., Mohammedi, K.: Contribution to the modeling and simulation of solar power tower plants using energy analysis. *Energy Convers. Manag.* **78**, 923–930 (2014). <https://doi.org/10.1016/j.enconman.2013.08.066>
44. Hezaveh, S.A., Farahani, S.D., Alibeigi, M.: Technical-economic analysis of the organic rankine cycle with different energy sources. *J. Solar Energy Res.* **5**(1), 362–373 (2020). <https://doi.org/10.22059/JSER.2020.300111.1148>
45. Mehmood, S., Reddy, B.V., Rosen, M.A.: Energy analysis of a biomass co-firing based pulverized coal power generation system. *Sustainability* **4**(4), 462–490 (2012). <https://doi.org/10.3390/su4040462>
46. Mann, M.K., Spath, P.L.: *Life cycle assessment of a biomass gasification combined-cycle power system: national renewable Energy Lab.*, Golden, CO (US) (1997)
47. Darrow, K., Tidball, R., Wang, J., Hampson, A.: *Catalog of CHP Technologies*, pp. 5–6. US Environmental Protection Agency, Washington (2015)
48. Wang, X., Yang, Y., Zheng, Y., Dai, Y.: Exergy and exergoeconomic analyses of a supercritical CO₂ cycle for a cogeneration application. *Energy* **119**, 971–982 (2017). <https://doi.org/10.1016/j.energy.2016.11.044>
49. Obidziński, S.A.: Pelletization of biomass waste with potato pulp content. *Int. Agrophys.* **28**(1), 85 (2014). <https://doi.org/10.2478/intag-2013-0030>
50. Kolb, G.J., Ho, C.K., Mancini, T.R., Gary, J.A.: *Power tower technology roadmap and cost reduction plan*. SAND2011-2419, Sandia National Laboratories, Albuquerque, NM. (2011) <https://doi.org/10.2172/1011644>
51. Fritsch, A., Frantz, C., Uhlig, R.: Techno-economic analysis of solar thermal power plants using liquid sodium as heat transfer fluid. *Sol. Energy* **177**, 155–162 (2019). <https://doi.org/10.1016/j.solener.2018.10.005>
52. Ghorbani, N., Aghahosseini, A., Breyer, C.: Assessment of a cost-optimal power system fully based on renewable energy for Iran by 2050—Achieving zero greenhouse gas emissions and overcoming the water crisis. *Renew. Energy* **146**, 125–148 (2020). <https://doi.org/10.1016/j.renene.2019.06.079>
53. Charbonneau, P., Knapp, B.: *A user's guide to PIKAIA 1.0*. (1995)

Publisher's Note Springer Nature remains neutral with regard to jurisdictional claims in published maps and institutional affiliations.

